PCT WORLD INTELLECTUAL PROPERTY ORGANIZATION
International Bureau

INTERNATIONAL APPLICATION PUBLISHED UNDER THE PATENT COOPERATION TREATY (PCT)

(51) International Patent Classification 6 : H04L

A2

(11) International Publication Number: **WO 97/21292**

(43) International Publication Date: 12 June 1997 (12.06.97)

(21) International Application Number: PCT/US96/18824

(22) International Filing Date: 22 November 1996 (22.11.96)

(30) Priority Data:
60/007,469 22 November 1995 (22.11.95) US
60/007,475 22 November 1995 (22.11.95) US

(71)(72) Applicant and Inventor: YANG, Lin-Lang [-/US]; 9979 Riverhead Drive, San Diego, CA 92129 (US).

(74) Agent: HARRIS, Scott, C.; Fish & Richardson, P.C., Suite 1400, 4225 Executive Square, La Jolla, CA 92037 (US).

(81) Designated States: CN, JP, KR, US, European patent (AT, BE, CH, DE, DK, ES, FI, FR, GB, GR, IE, IT, LU, MC, NL, PT, SE).

Published
Without international search report and to be republished upon receipt of that report.

(54) Title: A MULTIUSER DETECTOR FOR CODE DIVISION MULTIPLE ACCESS SYSTEMS

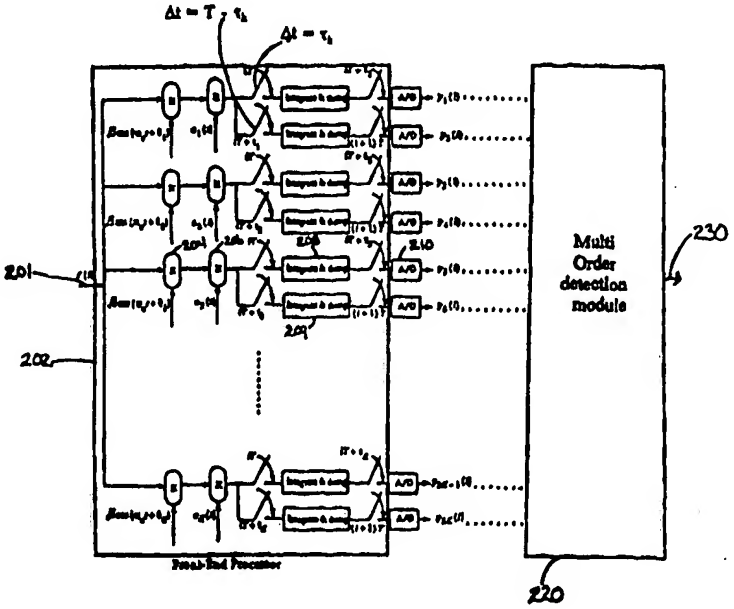

(57) Abstract

A multiuser detector for a CDMA system for real-time processing. Interference information of cross correlation from the signals of different users is processed to enhance the signal-to-noise ratio by suppressing the interference noise in a multiple-stage processing. A sampling processor is implemented to obtain at least two sets of data for each user with different integration times. The operation of the detector is dynamically adjusted to the operating condition of the CDMA system in a near real-time manner.

FOR THE PURPOSES OF INFORMATION ONLY

Codes used to identify States party to the PCT on the front pages of pamphlets publishing international applications under the PCT.

AM	Armenia	**GB**	United Kingdom	**MW**	Malawi
AT	Austria	**GE**	Georgia	**MX**	Mexico
AU	Australia	**GN**	Guinea	**NE**	Niger
BB	Barbados	**GR**	Greece	**NL**	Netherlands
BE	Belgium	**HU**	Hungary	**NO**	Norway
BF	Burkina Faso	**IE**	Ireland	**NZ**	New Zealand
BG	Bulgaria	**IT**	Italy	**PL**	Poland
BJ	Benin	**JP**	Japan	**PT**	Portugal
BR	Brazil	**KE**	Kenya	**RO**	Romania
BY	Belarus	**KG**	Kyrgystan	**RU**	Russian Federation
CA	Canada	**KP**	Democratic People's Republic of Korea	**SD**	Sudan
CF	Central African Republic			**SE**	Sweden
CG	Congo	**KR**	Republic of Korea	**SG**	Singapore
CH	Switzerland	**KZ**	Kazakhstan	**SI**	Slovenia
CI	Côte d'Ivoire	**LI**	Liechtenstein	**SK**	Slovakia
CM	Cameroon	**LK**	Sri Lanka	**SN**	Senegal
CN	China	**LR**	Liberia	**SZ**	Swaziland
CS	Czechoslovakia	**LT**	Lithuania	**TD**	Chad
CZ	Czech Republic	**LU**	Luxembourg	**TG**	Togo
DE	Germany	**LV**	Latvia	**TJ**	Tajikistan
DK	Denmark	**MC**	Monaco	**TT**	Trinidad and Tobago
EE	Estonia	**MD**	Republic of Moldova	**UA**	Ukraine
ES	Spain	**MG**	Madagascar	**UG**	Uganda
FI	Finland	**ML**	Mali	**US**	United States of America
FR	France	**MN**	Mongolia	**UZ**	Uzbekistan
GA	Gabon	**MR**	Mauritania	**VN**	Viet Nam

A MULTIUSER DETECTOR FOR CODE DIVISION MULTIPLE ACCESS SYSTEMS

This application claims the benefit of the U. S. Provisional Application No. 60/007,469, titled "Multiuser Detector for Multiple Access Communication System", filed on November 22, 1995, and 60/007,475, filed November 22, 1995, the disclosures of which are incorporated by reference.

FIELD OF THE INVENTION

The present invention relates to multiple access communication systems, and more specifically, to a detection system for code division multiple access systems.

BACKGROUND AND SUMMARY OF THE INVENTION

Code Division Multiple Access (CDMA) has emerged as a key technology for communication services. CDMA intentionally uses a transmission bandwidth that is usually several orders of magnitude larger than the minimum required signal or information bandwidth, e.g.,

the bandwidth implied by the basic message symbol rate in a communication system. The power of each user's signal is spread over a wide bandwidth. This results in low power spectral density and thereby the interference to another narrow band signal occupying the same frequency range is reduced. It also makes the presence of the signal less detectable to an invader.

A digital signal from each user in a CDMA system is modulated with a pseudo-noise (PN) binary sequence that is unique to that particular user. This modulation causes the spreading over the wide bandwidth. Each PN sequence appears random to a naive observer but can be reproduced in a deterministic manner by an intended receiver. Any two PN sequences are made substantially orthogonal to each other but some degree of cross correlation still exists. The mutual interference in the same frequency range of multiple users is greatly reduced in a CDMA system. This orthogonality allows multiple access within the same frequency spectrum and makes CDMA systems less vulnerable to intentional or unintentional interference. However, the cross correlation becomes limiting the system capacity as the number of users increases.

Detection of a CDMA system usually involves cross correlation with a locally-generated version of the PN

sequence. A desired user signal is generally detected by cross correlating with the exact same PN sequence that is uniquely assigned to that particular user by the system. Signals from other users contribute a small amount of wideband noise due to non-zero cross correlation value produced by the cross correlation operation.

The ratio of the transmission bandwidth over the information bandwidth indicates the degree of the spectrum spreading of a CDMA system. This ratio is often referred as the processing gain. Many beneficial properties of CDMA relate to the processing gain.

FIG. 1 shows a simplified CDMA system 100. User messages are modulated with a carrier frequency and decoded by PN sequence waveforms prior to transmission. A receiver system 130 process the received signals by filtering and correlation operation to recover the embedded user messages. A CDMA detector 137 is an essential part of the receiver 130.

CDMA systems have many unique properties. For example, multiple access communication by a large number of users in a common frequency range in the same and neighboring geographical areas are possible. This has particular significance in satellite and cellular communication systems. The number of simultaneous users

is usually proportional to the processing gain of the CDMA system. The efficiency of bandwidth usage of CDMA increases as the number of simultaneous users grows. The resistance to interference increases with the processing gain by suppressing the power in a narrow band. Adverse effects of multipath signals can be significantly reduced due to the spectrum spreading since only a small portion of signal will undergo fading at any given time. In addition, position location and velocity estimation can be measured with high accuracy in a CDMA system.

The application of CDMA in communication has been demonstrated in a number of systems in use including the IS-95 based CDMA cellular system disclosed in "On the Capacity of A Cellular CDMA System", by Gilhousen et al., IEEE Trans. Veh. Technol., Vol. VT-40(2), pp303-312, May, 1991, a PCS system based on IS-95, and the Globalstar LEO satellite system. The high capacity, high resolution time-of-arrival for positioning measurement, low probability of interception, and independent interference rejection makes CDMA communication systems one of the most promising candidates for multiuser communications.

The multiuser detection system is an important aspect of the CDMA technology. A portion of a simplified CDMA detection system is indicated by the signal mixers 133 and

135 and the detector 137 in FIG. 1. The CDMA detection system plays a substantially role in terms of the system capacity, processing speed, interference resistance, and noise reduction.

One significant limitation of the prior-art multiuser detectors in CDMA systems involves the cross-correlation information among users in signal detection. Many prior-art systems essentially neglect the cross correlation. This results in reduced error performance and consequently reduces the capacity of the system. This capacity loss is most significant when the processing gain of the system is high. Specifically, the cross correlation noise is not separated from the autocorrelated signal in many prior-art detectors.

Another limitation of the prior-art systems is the slow processing speed inherent in the detectors. This is partially due to the complexity of the prior-art decoder processing techniques. For example, Verdú first disclosed the idea of the optimal multiuser detector in "Minimum Probability of Error for Asynchronous Gaussian Multiple Access Channels", IEEE Trans. Inform. Theory, Vol. IT-32(1), pp.85-96, 1986. An ensemble of K received asynchronous signals as convolutional codes was used in the proposed system, where K is the number of users in the

system. The well-known Viterbi algorithm was used to decode these signals. Lupas and Verdú proved that Verdú's multiuser detector has a low bit error rate and is near-far resistant in "Near-Far Resistance of Multiuser Detectors in Asynchronous Channels", IEEE Trans. Comm, Vol.38(4), 1990. However, Verdú's scheme exhibited two major problems. First, the complexity of the system grows exponentially with the number of transmitted signals K. Even for a moderate value of K, Verdú's system is already hard to implement. Secondly, the whole period of the PN sequence is assumed to be modulated by only one symbol to reduce the computation, which makes the trellis become time invariant.

Most practical systems are usually designed with the whole period of the PN sequence being modulated by multiple data symbols. This makes the total complexity of Verdú's algorithm for binary phase shift keying (BPSK) waveforms to be 2^K plus the computation of the weight of 2×2^K branches in the trellis. Such complexity renders Verdú's system even less feasible. Verdú's system also requires information about the received power from each user in order to detect the received signals. In addition, effects due to multipath fading were not considered.

Several suboptimal multiuser detectors have been introduced after Verdú's detector, aiming at reducing the complexity of Verdú's system. For example, Xie et al. described a detector using sequential decoding in "Multiuser Signal Detection Using Sequential Decoding", IEEE Trans. Commm. Vol.38(5), pp.578-583, 1990. This system has a complexity proportional to K. Lupus and Verdú also disclosed a linear de-correlating detector with complexity proportional to K. However, both of the above systems make the same assumption as in Verdú's system, i.e., the whole period of the PN sequence is modulated by a single symbol.

Still another limitation of the prior-art multiuser detectors is the lack of capability of pipeline processing. The coded symbol signals are processed one at a time in each channel. A new coded symbol signal is accepted for decoding usually after the decoding of the previous symbol in the same channel is completed.

In view of the above limitations, a new type of multiuser detector with high capacity and fast processing speed is needed to improve the existing CDMA systems. In particular, separation of the cross correlation noise from the signal and reduction of the processing complexity are desirable.

The present invention describes an optimal multiuser detector with a dynamical system control at a high processing speed. Specifically, a double-sampling front-end processor is implemented in the preferred embodiment in accordance with the present invention. The detector further includes a dynamic control module for generating a system control δ-parameter based on the characteristics of the received signals, a correlation processor for processing cross correlation information of the received signals based on the δ-parameter, a plurality of approximation processors for recursively suppressing the cross correlation noise below a predetermined noise tolerance level based on the optimized δ-parameter, and a decision processor for generating the decoded data. The approximation processors form a plurality of substantially identical processing layers connected to each other in series. The correlation processor feeds information on both auto correlation and cross correlation of the input signals of multiple users to the first approximation processor in the series. In a preferred operation, received signals are processed layer by layer until the cross correlation noise is reduced below the predetermined level.

One aspect of the present invention is the linear dependence of the processing complexity with the number of the simultaneous users present in the system. This feature in combination with other unique properties of the preferred embodiment allows greater system capacity at faster processing speed in comparison with the prior-art systems.

Another aspect is the unique capability of pipeline processing mechanism. Each processing channel of the preferred embodiment is pipelined to increase the processing efficiency and speed in addition to the parallel processing implementation. In a preferred operation mode, a layer proceeds to accept and process a new signal upon completion of processing the previous data while the correlation processor feeds a new control δ-parameter adjusted and optimized for the new signal.

Still another aspect is the use of cross correlation information to substantially cancel the interference contributed by the cross correlation signals. This feature presents significant advantage over the prior-art system wherein the cross correlation signals is neglected as white noise. The minimized interference allows an increased system capacity of processing simultaneous users at the same and adjacent spatial locations.

Still another aspect is the dynamically adjusted system control for a high-speed convergence in the multi-layer processing. The detector of the preferred embodiment controls the decoding processing in each processing layer by feeding the layer with a dynamic control parameter δ. An optimized δ-parameter is preferably adjusted and determined individually by the characteristics of a received signal such as the number of the simultaneous users, K, the processing gain, the PN sequence, and the user delay. Generation of the δ-parameter is a simple digital operation at a high speed in the present invention.

Other aspects of the present invention include additional system enhancement by optimally combining the two output signals from the double-sampling front-end processor, digital generation of the PN sequence, and a mechanism for handling decoding process at very small user delay times relative to the signal bit duration.

The details of the preferred embodiment of the present invention are set forth in the accompanying drawings and the description below. Once the details of the invention are known, numerous additional innovations and changes will become obvious to one skilled in the art.

BRIEF DESCRIPTION OF THE DRAWINGS

FIG. 1 shows a block diagram of a simplified CDMA system.

FIG. 2 shows the preferred embodiment of the multiuser detector of the present invention with a circuitry for the front-end processor.

FIG. 3 illustrates the delay of each user signal and the corresponding transmitted data symbols during observation time from iT to $(i+1)T$.

FIG. 4 shows the δ-adjusted Mth order detection module in accordance with the present invention.

FIG. 5 shows the correlation processor.

FIG. 6 shows the approximation processor in accordance with the present invention.

FIG. 7 shows the decision processor in accordance with the present invention.

FIG. 8 illustrates the kth user's spectral-spreading signal, $a_k(t)$, during a observation time from iT to $(i+1)T$.

FIG. 9 shows the spectral-spreading signals, $a_k(t)$ and $a_l(t)$ for $\gamma_k = \gamma_l$ during a observation time from iT to $(i+1)T$.

FIG. 10 illustrates computation of $c_{mn}(i)$ for $\gamma_k > \gamma_l$.

FIG. 11 illustrates computation of $c_{mn}(i)$ for $\gamma_k<\gamma_1$.

FIG. 12 shows the process and the corresponding circuitry for obtaining $\cos(\theta_k-\theta_1)$.

FIG. 13 shows the magnitude of $V_{(2k-1)(21-1)}$, $V_{(2k-1)(21)}$, $V_{(2k)(21-1)}$, $V_{(2k)(21)}$ when $\gamma_k \leq \gamma_1$.

FIG. 14 shows the exact values of δ_{low} for β_k= 0dB.

FIG. 15 shows a comparison of the exact and approximated values of δ_{low}.

FIG. 16 shows the β_k as a function of K/N and δ for $\overline{g}_k$ =8.

FIG. 17 shows the β_k as a function of K/N and δ for $\overline{g}_k$=12.

FIG. 18 shows the β_k as a function of K/N and δ for $\overline{g}_k$=16.

FIG. 19 shows the β_k as a function of K/N and δ for $\overline{g}_k$=20.

FIG. 20 shows the β_k as a function of δ for K/N=0.2, 0.4, 0.6, and 0.8 and different values of $\overline{g}$.

FIG. 21 shows the contour of δ_{opt} as a function of K/N at different $\overline{g}$.

FIG. 22 shows the contour of exact and approximated values of δ_{opt} as a function of K/N at different $\overline{g}$.

FIG. 23 shows $\overline{\beta}_{opt}$ as a function of K/N for $\overline{g}$.

FIG. 24 shows a comparison of δ_{low} and δ_{opt}.

FIG. 25 shows $\overline{\beta}$ .versus δ for K/N=0.2, 0.4, 0.6, and 0.8.

FIG. 26 shows the results of the simulation of the symbol error rate probability for each user for the preferred embodiment of the multiuser detector.

FIG. 27 shows the simulated average symbol error probability of all users versus 3K/N in units of dB.

DETAILED DESCRIPTION OF THE INVENTION

The preferred embodiment and examples shown throughout this description should be considered as exemplars, rather than as limitations on the present invention. In particular, the mathematical formulas, equations and some assumptions contained herein are intended to illuminate the processes involved and functions of various system components or are used for clarity of discussion and should not be construed as limitations on the scope and contents of the invention.

Many features of the present invention are described in "Digital Algorithms for Multiuser Detector, Decision-Directed Phase Tracking Loop, and A/D & D/A Converter", a dissertation by Lin-Lang Yang, University of Southern California, December, 1995, the entirety of Chapter 1 and corresponding appendices of which are incorporated herewith by reference.

System Design of Multiuser Detector

FIG. 2 shows the preferred embodiment 200 of the multiuser detector of the present invention with a circuitry for the front-end processor 202. The detector

200 is a portion of the receiving system in an asynchronous direct sequence spread-spectrum multiple access system that is also known as a CDMA system. There are K users operating in an additive white Gaussian noise (AWGN) environment. A received analog signal 201, $r(t)$, at the input of the receiver is a sum of K spread-spectrum signals $s_k(t-\tau_k,b)$, wherein $1 \le k \le K$, and an AWGN random process, $n(t)$, with two-sided power spectrum density $N_o/2$:

$$r(t) = s(t,b) + n(t), \quad t \in R \tag{1}$$

where

$$s(t,b) = \sum_{k=1}^{K} s_k(t-\tau_k, b) = \sum_{i=0}^{L} \sum_{k=1}^{K} b_k(i)\, s_k(t - iT - \tau_k) \tag{2}$$

and

$$s_k(t) = \sqrt{2w_k}\, a_k(t) \cos(\omega_c t + \theta_k). \tag{3}$$

In the above equations, T denotes the symbol length which is the same for each of the K users, $s_k(t)$ is the waveform transmitted by the kth user during a T-second interval,

$a_k(t)$ is the kth user's spectral-spreading signal which is normalized to have unit power, τ_k is the time delay of the kth user, θ_k is the carrier phase of the kth user, ω_c is the common carrier frequency, w_k is the power of the kth user which is assumed constant for each user during the observation, $b_k(i)$ is the ith transmitted data symbol of the kth user with $b_k(i) \in \{-1,1\}$ for all k and i. and $(L+1)T$ is the message length for each user.

FIG. 3 shows an example of the delay of each user and the corresponding transmitted data symbols during observation time from iT to (i+1)T.

A preprocessor (not shown in FIG. 2) including a plurality of matched filters processes the composite signal 201 and decomposes it into corresponding K components for each user. Each component is sampled in the respect sampling channel in the front-end processor 202 and converted into digital signal by analog-to-digital converters 210. The output digital signals from the processor 202 are then subsequently decoded by the multiuser detection module 220 to recover the data symbols $b_k(i)$ from all K users embedded in the received signal 201.

The front-end processor 202 has K channels, one per user. Each channel includes a first signal mixer 204, a

second signal mixer 206, and two parallel integrate-and-dump detectors 208 and 209. The signal mixer 204 is used to demodulate the received signal at a common carrier frequency ω_c generated by a local oscillator. The carrier phase θ_k (k=1,2,...K) for each user is determined by a process (which will be described herein) and used for the demodulation. The second mixer 206 mixes the PN sequence generated the a local PN sequence generator with the received signal in each channel for further demodulation. When the carrier frequency ω_c, the carrier phase θ_k, the PN sequence epoch $a_k(t)$, and the symbol time for each user separately are synchronized through a synchronization process, the received signal r(t) is despread and demodulated by the local PN sequence and the local oscillator for each user. The K demodulated outputs are then integrated, sampled, and converted to digital signals for post-end signal processing.

According to the present invention, each channel are preferably sampled twice by two integration processes with different integration times. The first integrate-and-dump detector 208 for user k integrates for a duration of τ_k from time iT to time $iT+\tau_k$ and outputs value $y_{2k-1}(i)$. The second integrate-and-dump detector 209 for the same user k integrates for a duration of $(T-\tau_k)$ from time $iT+\tau_k$ to

time (i+1)T and outputs value $y_{2k}(i)$. Since each channel generates two output signals, a total of 2K signals are generated for K users by the double-sampling front-end processor 202. One advantage of this double sampling is to facilitate the implementation the novel multi-order detection module 220 for minimizing the cross correlation interference and pipelined processing.

The digital output signals $y_{2k}(i)$ and $y_{2k-1}(i)$ can be used to form a vector y(i) of 2K dimension:

$$y(i) \triangleq \begin{bmatrix} y_1(i) \\ y_2(i) \\ y_3(i) \\ y_4(i) \\ \vdots \\ y_{2K-1}(i) \\ y_{2K}(i) \end{bmatrix} \qquad (4)$$

Accordingly, the received data symbols $b_k(t)$ embedded in the received signal r(t) can also be defined in form of a vector z(i):

$$z(i) \triangleq \begin{bmatrix} \sqrt{w_1}b_1(i-1) \\ \sqrt{w_1}b_1(i) \\ \sqrt{w_2}b_2(i-1) \\ \sqrt{w_2}b_2(i) \\ \vdots \\ \sqrt{w_K}b_K(i-1) \\ \sqrt{w_K}b_K(i) \end{bmatrix} \tag{5}$$

Similarly, let vector $a_k(i, t)$ represent the waveform of the received PN sequence corresponding to $y(i)$:

$$a(t, i) \triangleq \begin{bmatrix} a_1(t, i) \\ a_2(t, i) \\ \vdots \\ a_{2K-1}(t, i) \\ a_{2K}(t, i) \end{bmatrix} \tag{6}$$

$$a_{2k-1}(t, i) = \begin{cases} a_k(t) \text{ if } iT \le t < iT + \tau_k, \\ 0 \quad otherwise, \end{cases}$$

$$a_{2k}(t, i) = \begin{cases} a_k(t) \text{ if } iT + \tau_k \le t < (i+1)T, \\ 0 \quad otherwise, \end{cases} \tag{7}$$

The correlation between $a_k(t,i)$ and $a_1(t,i)$ can be represented by $c_{k1}(i)$:

$$c_{k1}(i) = a_k(t,i) \bullet a_1(t,i) \triangleq \int_{iT}^{(i+1)T} a_k(t,i)\, a1(t,i)\, dt. \qquad (8)$$

A matrix $C(i)$ can be formed by $c_{k1}(i)$ to represent the correlation of the received PN sequence waveform:

$$C(i) = a(t,i) \bullet a'(t,i) \qquad (9)$$

where $a'(t,i)$ is the transpose matrix of $a(t,i)$.

The inventor found that ignoring the additive white Gaussian noise term, $n(t)$, can simplify the description without affecting the functionability of the preferred embodiment. The double frequency terms can also be filtered by the integrate-and-dump detectors 208 and 209. Thus, neglect of the AWGN and elimination of the double frequency terms lead to the following:

$$
\begin{aligned}
y_{2k-1}(i) &= \int_{iT}^{iT+\tau_k} r(t)\sqrt{2}\cos(\omega_{ct}+\theta_k)\,a_k(t)\,dt \\
&= \sqrt{w_k}b_k(i-1)\frac{T_k}{T} \\
&\quad + \sum_{l=1,\,l\neq k}^{K} \sqrt{w_l}b_l(i-1)\cos(\theta_k-\theta_l)\,c_{(2k-1)(2l-1)}(i) \\
&\quad + \sum_{l=1,\,l\neq k}^{K} \sqrt{w_l}b_l(i)\cos(\theta_k-\theta_l)\,c_{(2k-1)(2l)}(i)\,.
\end{aligned}
\tag{10}
$$

$$
\begin{aligned}
y_{2k}(i) &= \sqrt{w_k}b_k(i)\left(1-\frac{\tau_K}{T}\right) \\
&\quad + \sum_{l=1,\,l\neq k}^{K} \sqrt{w_k}b_l(i-1)\cos(\theta_K-\theta_l)\,c_{(2k)(2l-1)}(i) \\
&\quad + \sum_{l=1,\,l\neq k}^{K} b_l(i)\cos(\theta_K-\theta_l)\,c_{(2k)(2l)}(i)\,.
\end{aligned}
\tag{11}
$$

The above two equations can be written in vector form as

$$R(i)\,z(i) = y(i)\,, \tag{12}$$

where matrix $R(i)=[r_{kl}(i)]$ is given by

$$
\begin{aligned}
r_{(2k-1)(2k-1)}(i) &= \frac{\tau_k}{T}, \\
r_{(2k)(2k)}(i) &= 1 - \frac{\tau_k}{T}, \\
r_{(2k-1)(2k)}(i) &= 0, \\
r_{(2k)(2k-1)}(i) &= 0, \\
r_{(2k-1)(2l-1)}(i) &= \cos(\theta_k - \theta_l)\, c_{(2k-1)(2l-1)}(i), \\
r_{(2k-1)(2l)}(i) &= \cos(\theta_k - \theta_l)\, c_{(2k-1)(2l)}(i), \\
r_{(2k)(2l-1)}(i) &= \cos(\theta_k - \theta_l)\, c_{(2k)(2l-1)}(i), \\
r_{(2k)(2l)}(i) &= \cos(\theta_k - \theta_l)\, c_{(2k)(2l)}(i), \\
r_{kl}(i) &= r_{kl}(i).
\end{aligned}
\tag{13}
$$

Note that $r_{ll}(i)$ is independent of the data symbol index i, that is, $r_{ll}(i)$ is time invariant.

Equation (12) indicates that the received data vector $z(i)$ can be decoded from the sampled digital output vector $y(i)$ by the following operation:

$$z(i) = R(i)^{-1} y(i) \tag{14}$$

where $R(i)^{-1}$ is the inverse of $R(i)$.

Gaussian elimination is generally used to perform the operation of inversing a matrix. This is described, for example, by Strang in "Linear Algebra and Its

Application", 3rd edition, Harcout Brace Jovanovich, 1988. The matrix R(i) is a 2K x 2K matrix. The Gaussian elimination is known to require a number of $[(2K)^3 - 2K]/3$ "multiply-subtract" operations in forward elimination, and a number of $(2K)^2/2$ "multiply-subtract" operations in back-substitution. Therefore, a total number of

$$\frac{(2K)^3-2K}{3}+\frac{(2K)^2}{2}. \qquad (15)$$

operations is required. However, this number is usually too large for real time processing even when 2K is moderate. In addition, Gaussian elimination requires at least 2K serial operations in forward elimination, and at least 2K serial operation in back-substitution. This implies that the computation time will be lower bounded because of the number of serial operations required.

The inventor recognized the limitations of the conventional Gaussian elimination method and thereby devised a new approach to perform the matrix inverse operation shown in Equation (14). This new approach utilizes the small off-diagonal components inherent in the matrix *R(i)* to reduce the number of operations required by the Gaussian elimination. In particular, the reduced

number of operations in this new approach can be implemented using parallel processing. The new approach in accordance with the present invention allows real-time processing of $z(i)$.

The multi-order detection module 220 of FIG. 2 is designed to perform the operation shown in equation (14) to recover the data symbols represented by vector $z(i)$ from the sampled digital output vector y(i). The new approach of obtaining $R(i)^{-1}$ is implemented.

Multi-Order Approximation Processing

The preferred embodiment decomposes the matrix $R(i)$ into two parts, an diagonal matrix $D = [d_{ii}]$ containing only the diagonal components of $R(i)$ and a matrix Of containing only the off-diagonal components of $R(i)$. This can be expressed as the following:

$$R = D + O_f. \qquad (16)$$

$$d_{(2k-1)(2k-1)} = r_{(2k-1)(2k-1)} = \frac{\tau_k}{T}$$
$$d_{(2k)(2k)} = r_{(2k)(2k)} = 1 - \frac{\tau_k}{T}. \qquad (17)$$

An approximation processing method is used in the preferred operation mode. A positive system control parameter $\delta > 0$ is introduced along with three matrices D_δ, O_δ, and F_δ:

$$D_\delta = (1+\delta) D,$$
$$O_\delta = O_f - \delta D, \qquad (18)$$
$$F_\delta = D_\delta^{-1} O_\delta,$$

The parameter δ is dynamically adjusted based on the operation state of the CDMA system. The choice of a non-zero δ is to ensure the convergence of the processing. It is known that matrix F_δ for $\delta=0$ is not necessarily a convergent matrix. Optimization of δ parameter will make

the convergent speed faster. This will become apparent later.

The matrix R can be further decomposed in terms of D_δ and F_δ:

$$\begin{aligned} R &= D + O_f \\ &= (1+\delta) D\left(I + \frac{1}{1+\delta} D^{-1} O_f \right) - \delta D \\ &= (1+\delta) D\left(I - \frac{\delta}{1+\delta} I + \frac{1}{1+\delta} D^{-1} O_f \right) \\ &= (1+\delta) D\left(I + \frac{1}{1+\delta} D^{-1} O_f - \delta D \right) \\ &= D_\delta (I + D_\delta^{-1} O_\delta) \\ &= D_\delta (I + F_\delta) , \end{aligned} \tag{19}$$

where I is the identity matrix. The equation (12) can be written as

$$D_\delta (I + F_\delta) z = y . \tag{20}$$

The preferred approximation operation can be further represented by a matrix $H^{(M)}$ and an estimated

representation of the data symbol vector $z(i)$, $Z^{(M)}=[Z_1^{(M)}]$, both of which are defined as:

$$H^{(M)} \triangleq \left(\sum_{m=0}^{M} (-1)^m F_\delta^m\right) D_\delta^{-1},$$
$$\hat{z}^{(M)} \triangleq H^{(M)} y. \tag{21}$$

The integer, M=0, 1, 2, 3,..., is the order of approximation processing.

The relation of $z(i)$ and $Z^{(M)}$ is given by:

$$\begin{aligned} z^{(M)} &= H^{(M)} y \\ &= \left(\sum_{m=0}^{M} (-1)^m F_\delta^m\right) D_\delta^{-1} D_\delta (I + F_\delta) z \\ &= (I - (-1)^{M+1} F_\delta^{M+1}) z \\ &= z - (-1)^{M+1} F_\delta^{M+1} z \end{aligned} \tag{22}$$

Accordingly, the received data $b_k(i)$ can also be represented by an estimated $b_k^{(M)}(i)$. The estimated $b_k^{(M)}(i)$ can be determined by either $z_{2K}^{(M)}(i)$ or $z_{2K-1}^{(M)}(i+1)$.

A common practice in implementing CDMA systems is power control to ensure a substantially equal power distribution in the signals form K users. Implementation

of such power control will be assumed herein, i.e., w_k (k=1, 2, ..., K) for K users in Equation (3) is a constant denoted by w.

The inventor recognized that the integration times for obtaining digital output $y_{2k}(i)$ and $y_{2k-1}(i)$ for the kth user are different and therefore different weighting factors should be applied in combining the output signals $y_{2k}(i)$ and $y_{2k-1}(i)$. A combining ratio ξ is therefore optimally obtained in implementing the approximation processing of $Z(i)$. This combining ratio significantly affects the performance of the multiuser detector 200 in accordance with the present invention. The optimized value, ξ, also called maximal signal combining ratio, is achieved through a zeroth order approximation but will be used for all of orders in the preferred embodiment of the present invention.

It will be shown that the maximal signal combining ratio ξ is given by $(T-\tau_k)/T$. Therefore, the estimated $z_{2K}^{(M)}(i)$ is weighted by $\xi=(T-\tau_k)/T$, while the estimated $z_{2K-1}^{(M)}(i+1)$ is weighted by $(1-\xi)=\tau_k/T$. Accordingly, the received data estimated $b_k^{(M)}(i)$ for the kth user of the ith symbol can be expressed as

$$b_k^{(M)}(i) = \frac{T-\tau_k}{T}\frac{1}{\sqrt{\omega}}\hat{z}_{2k}^{(M)}(i) + \frac{\tau_k}{T}\frac{1}{\sqrt{\omega}}\hat{z}_{2k-1}^{(M)}(i+1) \qquad (23)$$

where the estimation noise $n_{bk}^{(M)}$ is defined as function of $F_d^m(i)=[f_{ij}^{(m)}(i)]$ by

$$\begin{aligned} {}^{(M)}_{b_k}(i) \triangleq -(-1)^{M+1}\Bigg(& \frac{T-\tau_k}{T}\sum_{j=1}^{K} f_{(2k)(2j-1)}^{(M+1)}(i)\, b_j(i-1) \\ & + \sum_{j=1}^{K}\left(\frac{T-\tau_k}{T} f_{(2k)(2j)}^{(M+1)}(i) + \frac{\tau_k}{T} f_{(2k-1)(2j-1)}^{(M+1)}(i+1)\right) b_j(i) \\ & = \frac{\tau_k}{T}\sum_{j=1}^{K} f_{(2k-1)(2j)}^{(M+1)}(i+1)\, b_j(i+1)\Bigg) \end{aligned} \qquad (24)$$

The estimation noise $n_{bk}^{(M)}$ is the interference contribution from the cross correlation of the signals from all other $(K-1)$ users except the kth user. Many prior-art CDMA systems simply neglect this estimation noise $n_{bk}^{(M)}$ as white noise in the background and consequently the resistance to the interference is compromised. This further adversely affect the maximal number of simultaneous users that the CDMA system can handle.

The multiuser detector 200 of the preferred embodiment uniquely processes the cross correlation

information and operates to minimize the corresponding noise. One aspect of the present invention is to use the dynamically adjusted and optimized δ parameter to ensure the convergence of the estimation noise $n_{bk}^{(M)}$, i.e.,

$$E\{(n_{bk}^{M+1)}(i))^2\} < E\{(n_{bk}^{(M)}(i))^2\} \qquad \forall k,\ i,\ \text{and } M, \tag{25}$$

where E{} denotes the operation of expected value. In addition, the δ parameter is chosen to produce a fast convergence. Determination of the optimal δ value will be described hereafter. The estimation noise $n_{bk}^{(M)}$ contributes less variance to $b_k^{(M)}(i)$ as more orders of the approximation processing are performed. The exact number of orders, M, for a particular CDMA system is determined by the maximal interference tolerance thereof.

Define a new set of vectors $z^{(M),wt}(i)=[z_1^{(M),wt}(i)]$, $x^{(M)}$, $s^{(M)}$ as the following:

$$\hat{z}^{(M),wt}(i) = D_\delta(i)H^{(M)}(i)y(i). \tag{26}$$

$$x^{(M)} = \left(O_\delta D_\delta^{-1}\right)^M y,$$
$$s^{(M)} = \sum_{m=0}^{M} (-1)^m x^{(m)}. \qquad (27)$$

The estimated $b_k^{(M)}(i)$ can be expressed as

$$\begin{aligned} b_k^{(M)}(i) &= \frac{T-\tau_k}{T}\frac{1}{\sqrt{w}} z_{2k}^{(M)}(i) + \frac{\tau_k}{T}\frac{1}{\sqrt{w}} z_{2k-1}^{(M)}(i+1) \\ &= \frac{(1+\delta)(T-\tau_k)}{(1+\delta)T}\frac{1}{\sqrt{w}} z_{2k}^{(M)}(i) + \frac{(1+\delta)\tau_k}{(1+\delta)T}\frac{1}{\sqrt{w}} z_{2k-1}^{(M)}(i+1) \qquad (28) \\ &= \frac{1}{\sqrt{w}(1+\delta)}\left(z_{2k}^{(M),wt}(i) + z_{2k-1}^{(M),wt}(i+1)\right), \end{aligned}$$

The approximation method in accordance with the present invention can now be revealed by the equation (28), which includes the following steps:

1. Compute the vector $z^{(M),wt}(i)$ as follows:

$$
\begin{aligned}
z^{(M),wt}(i) &= D_\delta(i)\, H^{(M)}(i)\, y(i) \\
&= \left(\sum_{m=0}^{M} (-1)^m (O_\delta(i)\, D_\delta^{-1}(i))^m \right) y(i) \\
&\triangleq \sum_{m=0}^{M} (-1)^m x^{(m)} \\
&\triangleq s^{(M)}.
\end{aligned}
\tag{29}
$$

2. Determine values of $b_k^{(M)}(i)$ for the kth user as follows:

$$
\begin{aligned}
&\text{If } z_{2k}^{(M),wt}(i) + z_{2k-1}^{(M),wt}(i+1) > 0, \text{ then } b_k^{(M)}(i) = +1; \\
&\text{If } z_{2k}^{(M),wt}(i) + z_{2k-1}^{(M),wt}(i+1) \le 0, \text{ then } b_k^{(M)}(i) = -1.
\end{aligned}
\tag{30}
$$

A recursion of $x^{(M)}$ and $s^{(M)}$ can be readily established from Equation (29):

$$
\begin{aligned}
x^{(M+1)} &= O_\delta D_\delta^{-1} x^{(M)}, \\
s^{(M+1)} &= s^{(M)} + (-1)^{M+1} x^{(M+1)},
\end{aligned}
\tag{31}
$$

wherein

$$x^{(0)} = y,$$
$$s^{(0)} = y. \qquad (32)$$

Therefore, the estimated $z^{(M),wc}(i)$ in Mth order can be extracted from the (M-1)th order of $s^{(M-1)}$ according to Equation (29) and Equation (31).

FIG. 4 shows a preferred implementation of the multi-order detector module 220 in the detector 200. The detector module 220 includes multi-order processing layers to implement the recursion processes in the above-described approximation method. The detector module 220 includes four sections, a correlation processor 410, a δ-generator 440, an approximation processor block 420 having a plurality of approximation processors 422, and a decision processor 430.

The δ-generator 440 monitors the operation status of the CDMA system and produces an optimized δ for each pair of the input signals 412 and 414 to the zeroth order approximation processor (in fact, they are identical to each other). The optimized δ to the correlation processor 410 automatically changes with operation status of the CDMA system. This dynamic mechanism is to keep the processing efficiency and speed at optimal.

The correlation processor 410 processes cross correlation information based on the PN sequence $a(t,i)$ 402, relative phase difference between users 404, i.e., $cos(\theta_k-\theta_l)$, and the dynamically adjusted δ value 442. FIG. 5 further illustrates the main tasks performed by the correlation processor 410 including computing the matrix $R(i)$, and computing the matrix D_δ. The information of the autocorrelation is included in the output matrix D_δ and the information of the cross correlation of different users is included in the output matrix O_δ. Both output signals D_δ and O_δ are δ-dependent and thereby are dynamically adjusted to the status change of the CDMA system.

The output signals from the correlation processor 410 are fed to the approximation processor block 420 to generate an output $S^{(M)}$ 424 with a minimized interference due to cross correlation of different users. A plurality of substantially identical approximation processors 422 are connected in series relative to each other to form multiple processing stages. As described previously, the δ is so chosen to ensure fast convergence of the multi-order processing so that the estimation noise $n_{bk}^{(M)}$ decreases as M increases. FIG. 6 further illustrates the operation of the approximation processor 422.

One unique feature of the approximation processor block 420 is the capability of continuous processing in a pipeline fashion. Each processor 422 at jth stage accepts and starts processing a new set of data from (j-1)th stage upon completion of feed previous set of data from (j-1)th stage to the next stage (j+1). Few prior-art systems implement such pipeline operation. The pipeline operation allows significant enhancement in processing efficiency and speed, thereby making the real-time implementation of multiuser detector feasible.

The approximation processor block 420 feeds the resulting signal $s^{(M)}$ to the decision processor 430 if the noise level from the cross correlation is reduced below a pre-set tolerance level. The operation of the decision processor 430 is illustrated in FIG. 7.

The above-described processors and the operations thereof can be implemented with the existing electronic circuitry and VLSI technology.

Correlation Processing and Correlation Matrix *R*

Signal decoding and detection by correlation operation is a known and widely used processing technique. The complexity of the correlation process usually

increases significantly with the number of simultaneous users present in a CDMA system. The necessary processing or computation often makes real-time processing impractical with the current digital technology. The preferred embodiment uses a new and unobvious approach to reduce the complexity of the such correlation processing by processing the auto correlation and cross correlation in a unique way. This is partially shown in the correlation matrix $R(i)$ that organizes the correlation information for further processing.

The correlation matrix $R(i)$ is defined by Equations (12) and (13). Information about the matrix $C(i)$ and $\cos(\theta_k-\theta_1)$ are needed in order to obtain the matrix $R(i)$ at the receiver.

In CDMA technology, a symbol bit is spectrally spread by the spectral-spreading signal waveform of a square wave $p(t)$. A single pulse of the PN waveform $p(t)$ is called a chip. The chip duration T_c determines the symbol processing gain N:

$$\textit{Processing gain} \quad N = \frac{T}{T_c} \tag{33}$$

The spectral spreading signal for the kth user (normalized to have unit power), $a_k(t)$, over a T-second interval can be expressed as the following:

$$a_k(t) = \sum_{n=0}^{LN} \frac{1}{\sqrt{T}} u_k(n) p(t - nT_c - Y_k) \quad (34)$$

where $u_k(n)$ is the nth transmitted chip of the kth user with $u_k(n) \in \{-1, 1\}$ and Y_k is the chip delay of the kth user where $Y_k = \tau_k \bmod T_c$. The waveform $a_k(t)$ is illustrated in FIG. 8.

The computation of the correlation matrix $C(i)$ is preferably obtained digitally in accordance with the present invention. This is due to the special structure of the above spectral-spreading signal $a_k(t)$. A digital circuitry suitable for generating such function is well-known in the art. Digital generation provides higher stability than the analog counterparts at lower cost.

Let the chip sequence, $sh_k(i)$, of length N+1 for the kth user between time iT and (i+1)T be defined by

$$sh_k(i) = \{u_k(iN-1), u_k(iN), u_k(iN+1), \cdots, u_k((i+1)N-1)\}. \quad (35)$$

In addition, let $sh_k^{RT}(i)$ denote the right-shifted version of $sh_k(i)$, that is,

$$sh_k^{RT}(i) = sh_k(i) \rightarrow 1 = \{u_k(iN-2), u_k(iN-1), u_k(iN), \cdots, u_k((i+)N-2)\} \quad (36)$$

where ->j denotes right-shift by j chips. If the chip delays γ_k and γ_l are both the same as shown in FIG. 9, then it is straightforward that $c_{(2k-1)(2l-1)}(i)$, $c_{(2k-1)(2l)}(i)$, $c_{(2k)(2l-1)}(i)$, and $c_{(2k)(2l)}(i)$ are functions of $sh_k(i) \oplus sh_l(i)$, τ_k and τ_l, where $\oplus$ denotes the exclusive or operator. The calculation of $sh_k(i) \oplus sh_l(i)$ can be implemented in VLSI technology. This is well known to the art.

Furthermore, most of the computation involved in the above derivation is merely the sum of random +1 and -1 plus the fractional chip correlation at the edge. The sum of random +1 and -1 only takes a very small amount of computation time in digital signal processing. This is one reason the preferred embodiment uses digital implementation for generating R.

In the case that $\gamma_k > \gamma_l$, the preferred embodiment first operates to move $a_k(t)$ leftwards in time domain by

an amount of $(\gamma_k - \gamma_l)$ to achieve chip alignment. This is to calculate the correlation values digitally. In this case, the correlation thus obtained is represented by

$$c_{mn}^{LT}(i) \tag{37}$$

with m = 2k-1, 2k and n = 2l-1, 2l. The variable $c_{mn}^{LT}(i)$ is a function of $sh_k(i) \oplus sh_l(i)$.

Secondly, the preferred embodiment first operates to shift $a_k(t)$ rightwards in time by an amount of $T_c - (\gamma_k - \gamma_l)$ and the corresponding correlation thus obtained is represented by

$$c_{mn}^{RT}(i), \tag{38}$$

in this case, $c_{mn}^{RT}(i)$ is a function of $sh_k^{RT}(i) \oplus sh_l(i)$. It is observed that the exact correlation value is given by

$$c_{mn}(i) = \alpha_{kl} c_{mn}^{LT}(i) + (1-\alpha_{kl})\, c_{mn}^{RT}(i) \tag{39}$$

where α_{kl} is given by

$$\alpha_{kl} = 1 - \left(\frac{Y_k}{T_c} - \frac{Y_l}{T_c} \right) \quad (40)$$

FIG. 10 illustrates the derivation of $c_{mn}(i)$ for $Y_k > Y_l$.

Similarly, when $Y_k < Y_l$, $a_l(t)$ is shifted first leftwards and then rightwards instead of moving $a_k(t)$. The corresponding correlation values thus obtained are denoted by $c_{mn}^{LT}(i)$ which is a function of $sh_l(i) \oplus sh_k(i)$ and $c_{mn}^{RT}(i)$ which is a function of $sh_l^{RT}(i) \oplus sh_k(i)$, respectively. Accordingly, the correlation value is given by

$$c_{mn}(i) = \alpha_{kl} c_{mn}^{LT}(i) + (1 - \alpha_{kl}) c_{mn}^{RT}(i) \quad (41)$$

$$\alpha_{kl} = 1 - \left(\frac{Y_l}{T_c} - \frac{Y_k}{T_c} \right) \quad (42)$$

This process is illustrated in FIG. 11.

It is concluded from Equations (40)~(42) that the correlation value can be generalized as

$$c_{mn}(i) = \alpha_{kl} c_{mn}^{LT}(i) + (1-\alpha_{kl})\, c_{mn}^{RT}(i) \qquad (43)$$

with m = 2k-1, 2k and n = 2l-1, 2l, where α_{kl} has value given by

$$\alpha_{kl} = 1 - \left| \frac{Y_l}{T_c} - \frac{Y_k}{T_c} \right|. \qquad (44)$$

In addition, the ones with larger chip delay shall be moved rightwards and leftwards. The cornerstone of the proposed multiuser detector is that the derivation of $c_{mn}^{LT}(i)$ and $c_{mn}^{RT}(i)$ mostly are the sum of random +1 and -1. This particular feature makes the characteristics of the matrix $R(i)$ readily obtainable digitally. Furthermore, a method of obtaining an approximation to the inverse of $R(i)$ can be determined based on the characteristics of $R(i)$.

FIG. 12 illustrates the circuitry and method for generation of $\cos(\theta_k-\theta_l)$ that are implemented in the preferred embodiment. A reference signal at the local oscillator frequency ω_c with a common reference phase θ_0 (an arbitrary real number) is generated for all K users in

the CDMA system. It is again assumed that the integration process will filter out all the terms with double frequency.

For the purpose of more concise notation, the system time index will be omitted mostly thereafter. Moreover, only time invariant symbol delays are considered.

Define Vmn as the time overlap between $a_n(t,i)$ and $a_m(t,i)$ in unit of chips. FIG. 13 illustrates examples of $V_{(2k-1)(2l-1)}$, $V_{(2k-1)(2l)}$, $V_{(2k)(2l-1)}$ and $V_{(2k)(2l)}$.

From Equation (13), it is observed that with time invariant symbol delay, the components $r_{(2k-1)(2k-1)}$, $r_{(2k)(2k)}$, $r_{(2k-1)(2k)}$, and $r_{(2k)(2k-1)}$ for k=1 to K, are all constants with values of

$$\begin{aligned} r_{(2k-1)(2k-1)} &= \frac{\tau_k}{T} = \frac{V_{(2k-1)(2k-1)}}{N}, \\ r_{(2k)(2k)} &= 1-\frac{\tau_k}{T} = \frac{V_{(2k)(2k)}}{N}, \\ r_{(2k-1(2k)} &= 0, \\ r_{(2k)(2k-1)} &= 0. \end{aligned} \tag{45}$$

Whereas, Equation (13) and Equation (43) indicate that $r_{(2k-1)(2l-1)}$ is a random variable with a value given by

$$r_{(2k-1)(2l-1)} = \cos(\theta_k-\theta)\, c_{(2k-1)(2l-1)} = \cos(\theta_k-\theta)\left(\alpha_{kl} c^{LT}_{(2k-1)(2l-1)} + (1-\alpha_{kl})\, c^{RT}_{2k-1)(2l-1)}\right). \quad (46)$$

In general, the probability distribution of θ_k and α_{kl}, and the relationship among random variables θ_k, θ_l, $c_{(2k-1)(2l-1)}$, α_{kl}, $c^{LT}_{(2k-1)(2l-1)}$, $c^{RT}_{(2k-1)(2l-1)}$ can be summarized as follows:

1. The random variable θ_k and θ_l are independent and identically distributed with uniform distribution between $-\pi$ and π, and they are independent of $c_{(2k-1)(2l-1)}$;

2. The random variable α_{kl} is uniformly distributed between 0 and 1, and is independent of $c^{LT}_{(2k-1)(2l-1)}$ and $c^{RT}_{(2k-1)(2l-1)}$.

The moments of $\cos(\theta_k-\theta_l)$ and α_{kl} can easily be calculated with the above relation:

$$\begin{aligned} E\{\cos(\theta_k-\theta_l)\} &= 0, \\ E\{\cos^2(\theta_k-\theta_l)\} &= \frac{1}{2}, \\ E\{\cos^4(\theta_k-\theta_l)\} &= \frac{3}{4}, \\ E\{\alpha_{kl}\} &= \frac{1}{2}, \\ E\{\alpha_{kl}^2\} &= \frac{1}{3}, \\ E\{\alpha_{kl}^4\} &= \frac{1}{5}, \end{aligned} \quad (47)$$

Assuming the chips in a PN sequence is independent identical distribution ("i.i.d") with equal probability to be +1 or -1, then the moments of $c_{(2k-1)(2l-1)}{}^{LT}$ and $c^{RT}{}_{(2k-1)(2l-1)}$ can be derived as shown in the following:

$$\begin{aligned} E\{c^{LT}_{(2k-1)(2l-1)}\} &= E\{c^{RT}_{2k-1)(2l-1)}\} = 0, \\ E\{(c^{LT}_{(2k-1)(2l-1)})^2\} &= E\{(c^{LT}_{2k-1)(2l-1)})^2\} \approx \frac{1}{N^2} V_{(2k-1)(2l-1)}, \\ E\{(c^{LT}_{(2k-1)(2l-1)})^4\} &= E\{(c^{LT}_{2k-1)(2l-1)})^4\} \\ &\approx \frac{1}{N^4}(3V^2_{2k-1)(2l-1)} - 2V_{(2k-1)(2l-1)}). \end{aligned} \tag{48}$$

and

$$\begin{aligned} E\{c^{LT}_{(2k-1)(2l-1)} c^{RT}_{(2k-1)(2l-1)}\} &= 0, \\ \{(c^{LT}_{(2k-1)(2l-1)})^2 (c^{RT}_{(2k-1)(2l-1)})^2\} &= \frac{1}{N^4} v^{2(2k-1)(2l-1)}, \\ \{(c^{LT}_{(2k-1)(2l-1)})^1 (c^{RT}_{(2k-1)(2l-1)})^3\} &= E\{(c^{LT}_{(2k-1)(2l-1)})^3 (c^{RT}_{(2k-1)(2l-1)})^1 \\ &= 0, \end{aligned} \tag{49}$$

Therefore, the moments of $r_{(2k-1)(2l-1)}$ and r_{lk} are given by

$$E\{r_{(2k-1)(2l-1)}\} = 0,$$
$$E\{r^2_{(2k-1)(2l-1)}\} = \frac{1}{3N^2} V_{(2k-1)(2l-1)}, \quad (50)$$
$$E\{r^4_{(2k-1)(2l-1)}\} = \frac{1}{N^4}\left(\frac{54}{40} V^2_{(2k-1)(2l-1)} - \frac{3}{10} V_{(2k-1)(2l-1)}\right);$$

and

$$E\{r_{1k}\} = 0,$$
$$E\{r^2_{1k}\} = \frac{1}{3N^2} V_{1k}, \quad (51)$$
$$E\{r^4_{1k}\} = \frac{1}{N^4}\left(\frac{55}{40} V^2_{1k} - \frac{3}{10} V_{1k}\right).$$

Matrix F_δ represents information of the off-diagonal elements of the correlation matrix $R(i)$. F_δ is δ-dependent and allows optimal control of the correlation processing in minimizing the interference. Each components in F_δ and F_δ^2 can be expressed as

$$f_{kk}^{(1)} = -\frac{\delta}{1+\delta},$$

$$f_{kk}^{(1)} = \frac{\delta}{1+\delta}\frac{r_{kl}}{r_{kk}} \quad \text{for } k \neq l,$$

$$f_{kk}^{(2)} = -\frac{1}{(1+\delta)^2}\left(\delta^2 + \sum_{j=1, j\neq k}^{2K} \frac{r_{kj}^2}{r_{kk}r_{jj}}\right), \tag{52}$$

$$f_{kl}^{(2)} = \frac{1}{(1+\delta)^2}\left(-\delta r_{kl}\left(\frac{1}{r_{kk}} + \frac{1}{r_{ll}}\right) + \sum_{j=1, j\neq k, j\neq l}^{2K} \frac{r_{kj}r_{jl}}{r_{kk}r_{jj}}\right), \quad \text{for } k \neq l.$$

The first and second moment of $f_{kk}^{(1)}$, $f_{kl}^{(1)}$, $f_{kk}^{(2)}$, and $f_{kl}^{(2)}$ can be computed as follows:

$$
\begin{aligned}
E\{f_{kk}^{(1)}\} &= -\frac{\delta}{1+\delta}, \\
E\{f_{kl}^{(1)}\} &= 0, \\
E\{f_{kk}^{(2)}\} &= \frac{1}{(1+\delta)^2}\left(\delta^2 + \sum_{j=1, j\neq k}^{2K} \frac{1}{3}\frac{V_{kj}}{V_{kk}V_{jj}}\right), \\
E\{f_{kl}^{(2)}\} &= 0, \\
E\{(f_{kk}^{(1)})^2\} &= \frac{\delta^2}{(1+\delta)^2}, \\
E\{(f_{kl}^{(1)})^2\} &= \frac{1}{3}\frac{1}{(1+\delta)^2}\frac{V_{kl}}{V_{kk}^2}, \\
E\{(f_{kk}^{(2)})^2\} &= \frac{1}{(1+\delta)^4}\left(\left(\delta^2 + \frac{1}{V_{kk}}\sum_{j=1, j\neq k}^{2K}\frac{1}{3}\frac{V_{kj}}{V_{jj}}\right)^2\right. \\
&\quad \left. + \frac{1}{V_{kk}^2}\sum_{j=1, j\neq k}^{2K}\left(\frac{446}{360}\frac{V_{kj}^2}{V_{jj}^2}\right)\right), \\
E\{(f_{kl}^{(2)})^2\} &= \frac{1}{(1+\delta)^4}\left(\frac{1}{3}\delta^2 V_{kl}\left(\frac{1}{V_{kk}} + \frac{1}{V_{ll}}\right)^2\right. \\
&\quad \left. + \sum_{j=1, j\neq k, j\neq l}^{2K}\frac{1}{9}\frac{V_{kj}}{V_{kk}^2}\frac{V_{jl}}{V_{jj}^2}\right)
\end{aligned}
\tag{53}
$$

The following relation is observed in obtaining the above results:

$$E\{r_{kj}^2 r_{km}^2\} = E\{r_{kj}^2\}E\{r_{km}^2\}. \tag{54}$$

Determination of Maximal Signal-Combining Ratio

The maximal signal combining algorithm dictates the performance of the proposed system. Due to the complexity that is involved in deriving the combining ratio, the maximal signal combining ratio is calculated only for the zeroth order multiuser detector. The same combining ratio will be used for other orders of multiuser detector. Although such weighting ratio does not guarantee the maximal estimation signal-to-noise ratio for M ≥1, it avoids the totally intractable computation that can be involved. Furthermore, as M increases, the estimation noise will be dominant by the adjustment δ instead of the combining ratio ξ, therefore, it make sense to use the zeroth order combining ratio for all of the orders.

Suppose the estimation $b_k^{(M)}(i)$ is generated by

$$b_k^{(M)}(i) = \xi \frac{1}{\sqrt{W}} Z_{2k}^{(M)}(i) + (1-\xi) \frac{1}{\sqrt{W}} Z_{2k-1}^{(M)}(i+1) \triangleq b_k(i) + n_{bk,\zeta}^{(M)}(i) \quad (55)$$

where the estimation noise $n_{bk}^{(M)}(i)$ is given by

$$n_{b_{k,\ell}}^{(M)}(i) \triangleq -(-1)^{M+1}\Bigg(\xi \sum_{j=1}^{K} f_{(2k)(2j-1)}^{M+1)}(i)\, b_j(i-1) + \sum_{j=1}^{K} \Big(\xi f_{(2k)(2j)}^{(M+1)}(i) + (1-\xi) f_{(2k-1)(2j-1)}^{(M+1)}(i+1) \Big) b_j(i) + (1-\xi) \sum_{j=1}^{K} f_{(2k-1)(2j)}^{(M+1)}(i+1)\, b_j(i+1) \Bigg). \quad (56)$$

Then the zeroth order multiuser detector will have estimation signal-to-noise ratio, $SNR^{(0),k}(i)$, given by

$$SNR^{(0),k}(i) \triangleq \frac{E\{b_k^2(i)\}}{E\{(n_{b_{k,\ell}}^{(0)}(i))^2\}} = \frac{1}{\rho^{(0)}}, \quad (57)$$

$$\begin{aligned} \rho^{(0)} &= \sum_{j=1}^{K} \Big(E\{(\xi f_{(2k)(2j-1)}^{(1)}(i))^2\} + E\{(\xi f_{(2k)(2j)}^{(1)}(i))^2\} \\ &\quad + 2\xi(1-\zeta) E\{f_{(2k)(2j)}^{(1)}(i)\} E\{f_{(2k-1)(2j-1)}^{(1)}(i+1)\} \\ &\quad + E\{((1-\zeta) f_{(2k-1)(2j-1)}^{(1)}(i+1))^2\} \\ &\quad + E\{((1-\xi) f_{(2k-1)(2j)}^{(1)}(i+1))^2\} \Big) \\ &= \frac{1}{(1+\delta)^2} \left(\delta^2 + \frac{1}{3} \frac{K-1}{N} \left(\frac{\zeta^2}{\frac{V_{(2k)(2k)}}{N}} + \frac{(1-\xi)^2}{1 - \frac{V_{(2k)(2k)}}{N}} \right). \right) \end{aligned} \quad (58)$$

Maximizing $SNR^{(0),k}(i)$ is equivalent to minimizing $\rho^{(0)}$ which in turn is equivalent to minimizing the following term:

$$\frac{\xi^2}{\frac{V_{(2k)(2k)}}{N}} + \frac{(1-\xi)^2}{1-\frac{V_{(2k)(2k)}}{N}}. \tag{59}$$

which reaches its minimum value at ξ_{max}:

$$\xi_{max} = \frac{V_{(2k)(2k)}}{N}. \tag{60}$$

This is the same signal combining ratio that is used in Equations (23) and (24), i.e., $(T-\tau_k)/T$.

Although a similar procedure can be done for the second order multiuser detector to find the maximal signal combining ratio, it turns out that the combining ratio is a very complicated function of V_{kk} for i = 1, 2, 3,..., and 2K. Likewise, it is infeasible to calculate the precise $v^{(M)}$ for M ≥2 which implies that the exact maximal combining ratio is very difficult to obtain for M ≥2. Therefore, the maximal combining ratio of the zeroth order detector will be used for other orders as well.

Moreover, as M increases, the multiuser detector 200 relies on the adjustment δ to reduce the impact from $n_{bk}^{(M)}(i)$ instead of the combining ratio ξ.

Estimation Noise Variance $\sigma^{(M),k}$ and Optimization of δ

As discussed previously, the estimated $b_k^{(M)}(i)$ and the estimation noise $n_{bk}^{(M)}(i)$ are related by $b_k^{(M)}(i)=b_k(i)+n_{bk}^{(M)}(i)$ given by

$$\begin{aligned} n_{b_k}^{(M)}(i) &= -(-1)^{M+1}\left(\frac{T-\tau_k}{T}\sum_{j=1}^{K} f_{(2k)(2j-1)}^{(M+1)}(i)\, b_j(i-1) \right. \\ &\quad + \sum_{j=1}^{K}\left(\frac{T-\tau_k}{T} f_{(2k)(2j)}^{(M+1)}(i) + \frac{\tau_k}{T} f_{(2k-1)(2j-1)}^{(M+1)}(i+1) \right) b_j(i) \\ &\quad \left. + \frac{\tau_k}{T}\sum_{j=1}^{K} f_{(2k-1)(2j)}^{(M+1)}(i+1)\, b_j(i+1) \right) \\ &= -(-1)^{M+1}\sum_{j=1}^{K}\left(\frac{T-\tau_k}{T} f_{(2k)(2j-1)}^{(M+1)}(i)\, b_j(i-1) \right. \\ &\quad + \left(\frac{T-\tau_k}{T} f_{(2k)(2j)}^{(M+1)}(i) + \frac{\tau_k}{T} f_{(2k-1)(2j-1)}^{(M+1)}(i+1) \right) b_j(i) \\ &\quad \left. + \frac{\tau_k}{T} f_{(2k-1)(2j)}^{(M+1)}(i+1)\, b_j(i+1) \right) \end{aligned} \tag{61}$$

$\sigma^{(M),k}$ is defined as the estimation noise variance for user k that is generated by the Mth order multiuser detector:

$$
\begin{aligned}
\sigma^{(M),k} &\triangleq E\{(n_{b_k}^{(M)}(i))^2\} \\
&= E\left\{\left(-(-1)^{M+1} \sum_{j=1}^{K} \left(\frac{T-\tau_k}{T} f_{(2k)(2j-1)}^{(M+1)}(i)\, b_j(i-1) \right.\right.\right. \\
&\quad + \left(\frac{T-\tau_k}{T} f_{(2k)(2j)}^{(M+1)}(i) + \frac{\tau_k}{T} f_{(2k-1)(2j-1)}^{(M+1)}(i+1) \right) b_j(i) \\
&\quad \left.\left.\left. + \frac{\tau_k}{T} f_{(2k-1)(2j)}^{(M+1)}(i+1)\, b_j(i+1) \right) \right)^2 \right\} \\
&= \sum_{j=1}^{K} \left(E\left\{ \left(\frac{T-\tau_k}{T} f_{(2k)(2j-1)}^{(M+1)}(i) \right)^2 \right\} + E\left\{ \left(\frac{T-\tau_k}{T} f_{(2k)(2j)}^{(M+1)}(i) \right)^2 \right\} \right. \\
&\quad + 2\frac{\tau_k}{T}\frac{T-\tau_k}{T} E\{f_{(2k)(2j)}^{(M+1)}(i)\} E\{f_{(2k-1)(2j-1)}^{(M+1)}(i+1)\} \\
&\quad \left. + E\left\{ \left(\frac{\tau_k}{T} f_{(2k-1)(2j-1)}^{(M+1)}(i+1) \right)^2 \right\} + E\left\{ \left(\frac{\tau_k}{T} f_{(2k-1)(2j)}^{(M+1)}(i+1) \right)^2 \right\} \right) \\
&\triangleq \sum_{j=1}^{K} \sigma_j^{(M),k},
\end{aligned}
\tag{62}
$$

where $\sigma^{(M),k}$ denotes the estimation noise variance contributed by user j to user k in the Mth order multiuser detector and is given by

$$
\begin{aligned}
{}_{j}^{(M),k} &\triangleq E\left\{ \left(\frac{T-\tau_k}{T} f_{(2k)(2j-1)}^{(M+1)}(i) \right)^2 \right\} + E\left\{ \left(\frac{T-\tau_k}{T} f_{(2k)(2j)}^{(M+1)}(i) \right)^2 \right\} \\
&\quad + 2\frac{\tau_k}{T}\frac{T-\tau_k}{T} E\{f_{(2k)(2j)}^{(M+1)}(i)\} E\{f_{(2k-1)(2j-1)}^{(M+1)}(i+1)\} \\
&\quad + E\left\{ \left(\frac{\tau_k}{T} f_{(2k-1)(2j-1)}^{(M+1)}(i+1) \right)^2 \right\} \\
&\quad + E\left\{ \left(\frac{\tau_k}{T} f_{(2k-1)(2j)}^{(M+1)}(i+1) \right)^2 \right\}.
\end{aligned}
\tag{63}
$$

The order of the expectation and the summation in Equation (62) is exchangeable, because the received data of

different users are independent relative to each other. Also, it is assumed that the received data are equally likely to be +1 or -1, that the random variable $f_{kl}^{(M)}(i)$ is independent to the received data $b_j(i)$, and that the random matrix $F_\delta^{(M)}(i)$ is independent of the random matrix $F_\delta^{(M)}(l)$ when $i \neq l$.

Since the first and second moments of F_δ and F_δ^2 are available in Equation (53), $\sigma_j^{(0),k}$ and $\sigma_j^{(1),k}$ can be derived as the following:

$$
\begin{aligned}
\delta_k^{(0),k} &= \frac{\delta^2}{(1+\delta)^2} \\
\delta_{j,j\neq k}^{(0),k} &= \frac{1}{3N}\frac{1}{(1+\delta)^2}, \\
\delta_k^{(1),k} &\approx \frac{1}{(1+\delta)^4}\left(\delta^2 + \frac{2}{3}\frac{K}{N}\right)^2, \\
\delta_{j,j\neq k}^{(1),k} &= \frac{1}{(1+\delta)^4}\left(\frac{1}{N^2}\frac{2}{9}(K-2)\right. \\
&\qquad \left. + \frac{1}{N}\frac{\delta^2}{3} g\left(\frac{V_{(2k-1)(2k-1)}}{N}, \frac{V_{(2j-1)(2j-1)}}{N}\right)\right).
\end{aligned}
\tag{64}
$$

wherein

$$
\begin{aligned}
& g\left(\frac{V_{(2k-1)(2k-1)}}{N}, \frac{V_{(2j-1)(2j-1)}}{N}\right) \\
& \triangleq \frac{V_{(2k)(2j-1)}}{N}\left(1+\frac{\frac{V_{(2k)(2k)}}{N}}{\frac{V_{(2j-1)(2j-1)}}{N}}\right)^2 \\
& \quad + \frac{V_{(2k)(2j)}}{N}\left(1+\frac{\frac{V_{(2k)(2k)}}{N}}{\frac{V_{(2j-1)(2j-1)}}{N}}\right)^2 \\
& \quad + \frac{V_{(2k-1)(2j-1)}}{N}\left(1+\frac{\frac{V_{(2k-1)(2k-1)}}{N}}{\frac{V_{(2j-1)(2j-1)}}{N}}\right)^2 \\
& \quad + \frac{V_{(2k-1)(2j)}}{N}\left(1+\frac{\frac{V_{(2k-1)(2k-1)}}{N}}{\frac{V_{(2j)(2j)}}{N}}\right)^2 .
\end{aligned}
\tag{65}
$$

Special attention should be given to the user-independent second moment of the estimation noise, $\sigma_j^{(0),k}$ and $\sigma_j^{(1),k}$, when $\delta=0$. This particular structure happens when the proposed maximal signal combining algorithm is used.

The optimal value of δ for order M is the one that achieves the minimum estimation noise variance from all users, i.e.,

$$\delta_{opt}^{(M)} = \left\{ \delta : \min_{\delta} \sum_{k=1}^{K} \sigma^{(M),k} \right\}. \qquad (66)$$

Equation (64) indicates that the complexity of the estimation noise variance as a function of δ increases as the order increases. Therefore, it is very difficult to find an optimal value of δ for all orders.

The multiuser detector 200 of preferred embodiment instead searches for a δ which assures the fast convergence of the estimation noise. Moreover, the optimal value of δ should not be order-dependent or symbol-delay-dependent in order to reduce the implementation complexity.

Using Equation (62), it is found that the upper bound to the estimation noise variance is given by

$$\sigma^{(M),k} = \sum_{j=1}^{K} \left(E\left\{ \left(\frac{T-\tau_k}{T} f^{(M+1)}_{(2k)(2j-1)}(i) \right)^2 \right\} \right.$$

$$+ E\left\{ \left(\frac{t-\tau_k}{T} f^{(M+1)}_{(2k)(2j)}(i) \right)^2 \right\}$$

$$+2 \frac{\tau_k}{T} \frac{T-\tau_k}{T} E\{f^{(M+1)}_{(2k)(2j)}(i)\} E\{f^{(M+1)}_{(2k-1)(2j-1)}(i+1)\}$$

$$\left. + E\left\{ \left(\frac{\tau_k}{T} f^{(M+1)}_{(2k-1)(2j-1)}(i+1) \right)^2 \right\} \right. \qquad (67)$$

$$+E\left\{ \left(\frac{\tau_k}{T} f^{(M+1)}_{(2k-1)(2j)}(i+1) \right)^2 \right\}$$

$$\leq 2 \frac{\tau_k}{T} \frac{T-\tau_k}{T} E\{f^{(M+1)}_{(2k)(2k)}(i)\} E\{f^{(M+1)}_{(2k-1)(2k-1)}(i+1)\}$$

$$+\sigma^{(0),k} \sum_{j=1}^{2K} \sum_{l=1}^{2K} E\{f^{(M)}_{lj}\}$$

wherein $E\{f_{kl}^{(M)}\} = 0$ for $k \neq 1$.

When M is a moderately large number, the first term in Equation (67) will be much smaller than the second term when the estimation noise variance is a decreasing function of δ, i.e.,

$$2 \frac{\tau_k}{T} \frac{T-\tau_k}{T} E\{f^{(M+1)}_{(2k)(2k)}(i)\} E\{f^{(M+1)}_{(2k-1)(2k-1)}(i+1)\}$$

$$\ll \sigma^{(0),k} \sum_{j=1}^{2K} \sum_{l=1}^{2k} E\{f_{lj}^{M}\}. \qquad (68)$$

Therefore, the upper bound of the estimation noise variance $\sigma^{(M),k}$ can be approximated by

$$\sigma_{upper}^{(M),k} \approx \sigma^{(0),k} \sum_{j=1}^{2K} \sum_{l=1}^{2K} E\{f_{lj}^{(M)}\}. \quad (69)$$

Similarly, we can also derive the upper bound to the estimation noise variance $\sigma^{(M+1),k}$:

$$\sigma_{upper}^{(M+1),k} \approx \sigma^{(1),k} \sum_{j=1}^{2K} \sum_{l=1}^{2K} E\{f_{lj}^{(M)}\}. \quad (70)$$

It is desirable to find a δ value so that

$$\delta_{opt} = \left\{ \delta : \min_{\delta} \frac{\Sigma_{k=0}^{K} \sigma^{M+1,k}}{\Sigma_{k=0}^{K} \sigma^{(M),k}} \right\}, \quad (71)$$

which will allow the optimal decrease of estimation noise between two consecutive processing stages in the approximation processor block 420 shown in FIG. 4.

Since the close form of $\sigma^{(M),k}$ is very difficult to find, the δ-generator 440 shown in FIG. 4 is thus configured to obtain the optimal δ_{opt} by the following criterion instead,

$$\delta_{opt} = \left\{\delta : \min_{\delta} \frac{\Sigma_{k=0}^{K}\sigma_{upper}^{(M+1),k}}{\Sigma_{k=0}^{K}\sigma_{upper}^{(M),k}}\right\} = \left\{\delta : \min_{\delta} \frac{\Sigma_{k=0}^{K}\sigma^{(1),k}}{\Sigma_{k=0}^{K}\sigma^{(0),k}}\right. \tag{72}$$

The apability of serving a large number of simultaneous users is one of the advantages of a CDMA system. Therefore, it is reasonable to assume that the number of users, K, is much larger than 1, i.e., K >> 1. This assumption is used in the description herebelow.

The ratio of the estimation noise variance of the first order to that of the zeroth order for the kth user can be found as

$$\beta_k \triangleq \frac{\sigma^{(1),k}}{\sigma^{(o),k}}. \tag{73}$$

$$\beta_k = \frac{\sigma^{(1),k}}{\sigma^{(0),k}} = \frac{\Sigma_{j=1}^{K} \sigma_j^{(1),k}}{\Sigma_{j=1}^{K} \sigma_j^{(0),k}} \approx \frac{(\delta^2 + \frac{2}{3}\frac{K}{N})^2 + \frac{2}{9}(\frac{K}{N})^2 + \frac{1}{3}\delta^2 \frac{K}{N}\bar{g}_k}{(\delta^2 + \frac{1}{3}\frac{K}{N})(1+\delta)^2}, \quad (74)$$

wherein

$$\bar{g}_k = \frac{1}{K} \sum_{j=1, j\neq k}^{K} g\left(\frac{V_{(2k-1)(2k-1)}}{N}, \frac{V_{(2j-1)(2j-1)}}{N} \right). \quad (75)$$

It is desirable that β_k is less than 1 for all k in order to assure convergence of the preferred multiuser detector 200 in FIG. 2.

For the general case, δ shall satisfy:

$$\frac{(\delta+\frac{2}{3}\frac{K}{N})^2+\frac{2}{9}(\frac{K}{N})^2+\frac{1}{3}\delta^2\frac{K}{N}\bar{g}k}{(\delta^2+\frac{1}{3}\frac{K}{N})(1+\delta)^2}<1, \quad \forall k,$$

$$(\delta^2+\frac{2}{3}\frac{K}{N})^2+\frac{2}{9}(\frac{K}{N})^2+\frac{1}{3}\delta^2\frac{K}{N}\bar{g}k<(\delta^2+\frac{1}{3}\frac{K}{N})(1+\delta)^2, \tag{76}$$

$$\delta^3+(\frac{1}{2}-\frac{K}{2N}-\frac{1}{6}\frac{K}{N}\bar{g}k)\delta^2+\frac{1}{3}\frac{K}{N}\delta+\frac{1}{6}\frac{K}{N}-\frac{1}{3}(\frac{K}{N})^2>0.$$

The lower limit for δ is approximately given by

$$\delta_{low}\approx\frac{K}{2N}+\frac{1}{6}\frac{K}{N}\bar{g}k-\frac{1}{2}. \tag{77}$$

FIG. 14 shows the exact value of δ_{low} for $\bar{g}_k$=8, 12, 16, and 20. The exact value and the approximated value of δ_{low} are compared in FIG. 15 for $\bar{g}_k$=12 and 20.

FIGs 16-19 shows β_k (in dB) against K/N and δ for $\bar{g}_k$=8, 12, 16, and 20, respectively. It can be seen that the area above 0 dB increases with $\bar{g}_k$, especially for small δ and large K/N.

FIG. 20 shows the values of β_k (in dB) against δ for K/N=0.2, 0.4, 0.6, and 0.8.

It should be noted that $\bar{g}_k$ be bounded. Otherwise, β_k will easily exceed 0dB for large value of $\bar{g}_k$. This can be

understood by the result that the expectation value $E\{g(x,y)\}$ is large when x is close to zero and $\bar{g}_k$ will be close to $E\{g(x,y)\}$ for $x= V_{(2k-1)(2k-1)}/N$ when K is large. Therefore, one of the alternatives for avoiding a large $\bar{g}_k$ is to discard the information carried by very small V_{ll}.

For example, the information carried by $V_{ll} < \epsilon N$ where $\epsilon<<1$. In this case, the lth row and the lth column of matrices O_δ and D_δ^{-1} are set to zeros, and the lth component of vector y(i) is set to zero. Moreover, the combining ratio, ξ, in Equation (55) will be zero if l is an even number and 1 if l is an odd number.

Therefore, in a preferred operation of the multiuser detector 200 in FIG. 2, the output signals, $y_{2k-1}(i)$, from the integrate-and-dump detector 209 will be set to zero when the delay τ_k of the kth user is smaller than a threshold value, τ_{min}, since the filtering effect of the integration sampling process is substantially eliminated when $\tau_k<\tau_{min}$. One example of setting the threshold value τ_{min} is

$$\tau_{min}=\frac{T}{N}, \tag{78}$$

where T is the symbol bit duration and N is the processing gain.

The optimal δ value produces the minimum average value of β_k for all K users:

$$\begin{aligned}\bar{\beta}_{opt} &\triangleq \min_{\delta} \bar{\beta} \\ &= \min_{\delta} \frac{1}{K} \sum_{k=1}^{K} \beta_k \\ &= \min_{\delta} \frac{(\delta^2 + \frac{2}{3}\frac{K}{N})^2 + \frac{2}{9}(\frac{K}{N})^2 + \frac{1}{3}\delta^2 \frac{K}{N}\bar{g}}{(\delta^2 + \frac{1}{3}\frac{K}{N})(1+\delta)^2}.\end{aligned} \tag{79}$$

$$\bar{g} \triangleq \frac{1}{K} \sum_{k=1}^{K} \bar{g}_k. \tag{80}$$

which results in the following equation for δ_{opt}:

$$\begin{aligned}&\delta_{opt}^5 - \frac{K}{N}(1 + \frac{1}{3}\bar{g})\delta_{opt}^4 + \frac{2}{3}(\frac{K}{N})\delta_{opt}^3 \\ &-\frac{4}{3}(\frac{K}{N})^2 \delta_{opt}^2 + \frac{1}{9}(\frac{K}{N})^2 (\bar{g} - 2)\delta_{opt} - \frac{2}{9}(\frac{K}{N})^3 = 0.\end{aligned} \tag{81}$$

FIG. 21 shows δ_{opt} vs. K/N for different values of $\bar{g}$. It can be shown that δ_{opt} can be approximated by the following formula:

$$\delta_{opt} \approx \frac{K}{N}\left(1 + \frac{1}{3}\bar{g}\right) \qquad (82)$$

The exact value and the approximated value of δ_{opt} are compared in FIG. 22, which shows a small deviation.

The preferred embodiment of the present invention uses the approximated value of δ_{opt} of Equation (82) as a criterion for choosing an optimal the approximated value of δ_{opt}. Parameter $\bar{g}$ in Equation (82) usually does not change significantly. Hence, the optimal δ_{opt} is essentially a function of number of users, K, and the processing gain, N.

FIG. 23 shows the average $\bar{\beta}_{opt}$ in dB as a function of K/N for different values of $\bar{g}$. It is shown that $\bar{\beta}_{opt}$ can be as small as -5.5 dB for K/N=0.15. When K/N=1.1, $\bar{\beta}_{opt}$ still has a value of -1dB.

FIG. 24 compares δ_{opt} and δ_{low} in terms of K/N for different values of $\bar{g}$. It is shown that δ_{opt} satisfies the convergence requirement for $g_k \leq 16$.

FIG. 25 further shows that δ_{opt} indeed achieves the optimized value $\bar{\beta}_{opt}$ for K/N=0.2, 0.4, 0.6, and 0.8.

Simulation Results for Preferred Multiuser Detector

Several operation scenarios of the preferred multiuser detector 200 were stimulated to demonstrate the some aspects of the present invention.

It is assumed that each users' PN sequence is generated by using the following generator function,

$$g(x) = x^{42} + x^{35} + x^{33} + x^{31} + x^{27} + x^{26} + x^{25} + x^{22} + x^{21} + x^{19} + x^{18} + x^{17} + x^{16} + x^{10} + x^{7} + x^{6} + x^{5} + x^{4} + x^{3} + x^{2} + x + 1 \quad (83)$$

The symbol delay, τ_k, the received carrier phase, θ_k, and the transmitted data, $b_k(i)$, for all users are randomly generated. The input signal y(i) to the multi-order detector module 220 of FIG. 2 is obtained by using $R(i)z(i)=y(i)$.

A symbol data rate is subsequently generated by comparing the estimated data, $b_k^{(M)}(i)$ with the transmitted data, $b_k(i)$. FIG. 26 shows the symbol error rate of each user for the δ-adjusted Mth-order multiuser detector 200. Comparison are made for M=0, 2, and 4. Each data point is generated with 10^6 simulated symbols. In this simulation, the number of users in the system, K, is set to 40, and

the symbol processing gain, N, is 42. Moreover, the ϵ is set to 1/42=0.0238, i.e., any information carried in any interval shorter than 1 chip will be discarded. It can be shown that the variable $\bar{g}$ has a value of 6.9 for ϵ=1/42=0.0238. The optimal value of δ is approximately given by $\delta_{opt} = (K/N)(1+\bar{g}/3) = 3.143$ for $\bar{g}$=6.9.

FIG. 27 illustrates the average symbol error rate of all users against 3N/K in dB for M = 0, 2, 4, and 6. The parameters, except K and δ_{opt}, are set to the same values as in the first simulation shown in FIG. 26. Again, each point is generated with 10^6 simulated symbols.

FIG. 27 indicates that the system capacity increases as M increases. The system capacity is usually defined as the number of users that can be accommodated in a system with the average symbol error rate below some threshold value. For example, if the performance target is set to keep the average symbol error rate below 10^{-2}, then FIG. 27 shows that there is a capacity gain of about 2.5 dB for M = 2 as compared to M = 0.

The above described multiuser detector can also work for a system with inclusion of the background noise such as additive white Gaussian noise.

In addition, the present invention can also used to improve incoherent system. Many terrestrial wireless

applications use non-coherent detection because each user has independent random phase due to Rayleigh fading channel. The coherent detection can easily be used in forward link (base station to mobile station) detection in an IS-95 based CDMA cellular system because the existence of the pilot signal. The multiuser detector of the present invention can be used to cancel interference caused by signal from adjacent cells, especially when the mobile station is in a hand-off region.

A number of embodiments of the present invention have been described. Nevertheless, it will be understood that various modifications may be made without departing from the spirit and scope of the invention. Accordingly, it is to be understood that the invention is not to be limited by the specific illustrated embodiment, but only by the scope of the appended claims.

CLAIMS

What is claimed is:

1. An information processing system for detecting encoded signals of a plurality of users in a CDMA system, comprising:

a sampling processor, having a demodulating element and an integrating element for sampling said encoded signals, producing a plurality of digital signals indicative of said encoded signals; and

a detector, receiving signals from said sampling processor, having a correlator for performing a correlation of said encoded signals to obtain indicia of interference of said signals from different users and a processor for processing said indicia of interference in a predetermined way to substantially remove said interference from said detector.

2. A system as in claim 1, wherein said integrating element has a circuitry for sampling each of said encoded signals with at least two integration times.

3. A system as in claim 1, wherein said processor of said detector includes a plurality of processing modules connected in series, operating to sequentially process said encoded signals based on an approximation process, each of said processing modules responding to a system status parameter in a dynamic manner.

4. A method for minimizing interference of cross correlation of received signals from different users in a CDMA system, comprising:

sampling said received signals to obtain multiple representations of said signals based on coding information thereof;

processing said signals in said representations with a first correlation operation;

processing said signals with a second correlation operation subsequent to said first correlation operation, said second correlation

operation operating according to a operating condition of said CDMA system; and

performing a plurality of recursive operations to minimize said interference.

5. A signal improving device for a CDMA system, comprising:

a signal processing element, obtaining a CDMA signal, and processing said signal to determine a portion of said signal which represents interference;

a filter, removing at least a part of said portion of said signal that represents interference, to produce an interference-filtered signal; and

a recursion device, receiving said interference filtered signal, determining an amount of interference in said interference filtered signal, and sending said interference filtered signal through said signal processing element and said filter if an amount of interference in said interference filtered signal meets a specified criterion.

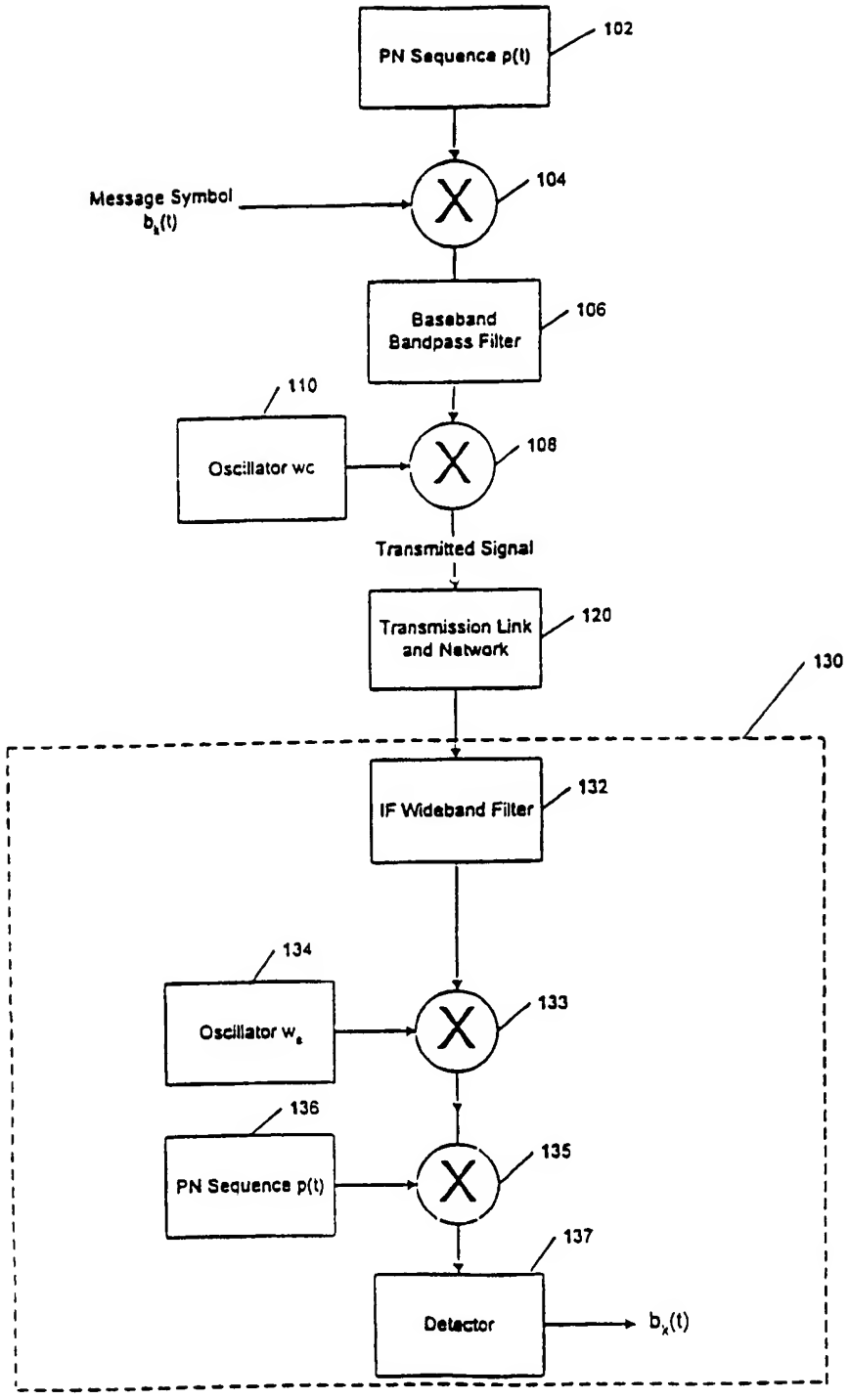
PN Sequence p(t)
102
Message Symbol
$b_k(t)$
104
Baseband
Bandpass Filter
106
110
Oscillator wc
108
Transmitted Signal
Transmission Link
and Network
120
130
IF Wideband Filter
132
134
Oscillator w_c
133
136
PN Sequence p(t)
135
137
Detector
$b_k(t)$

Figure 1

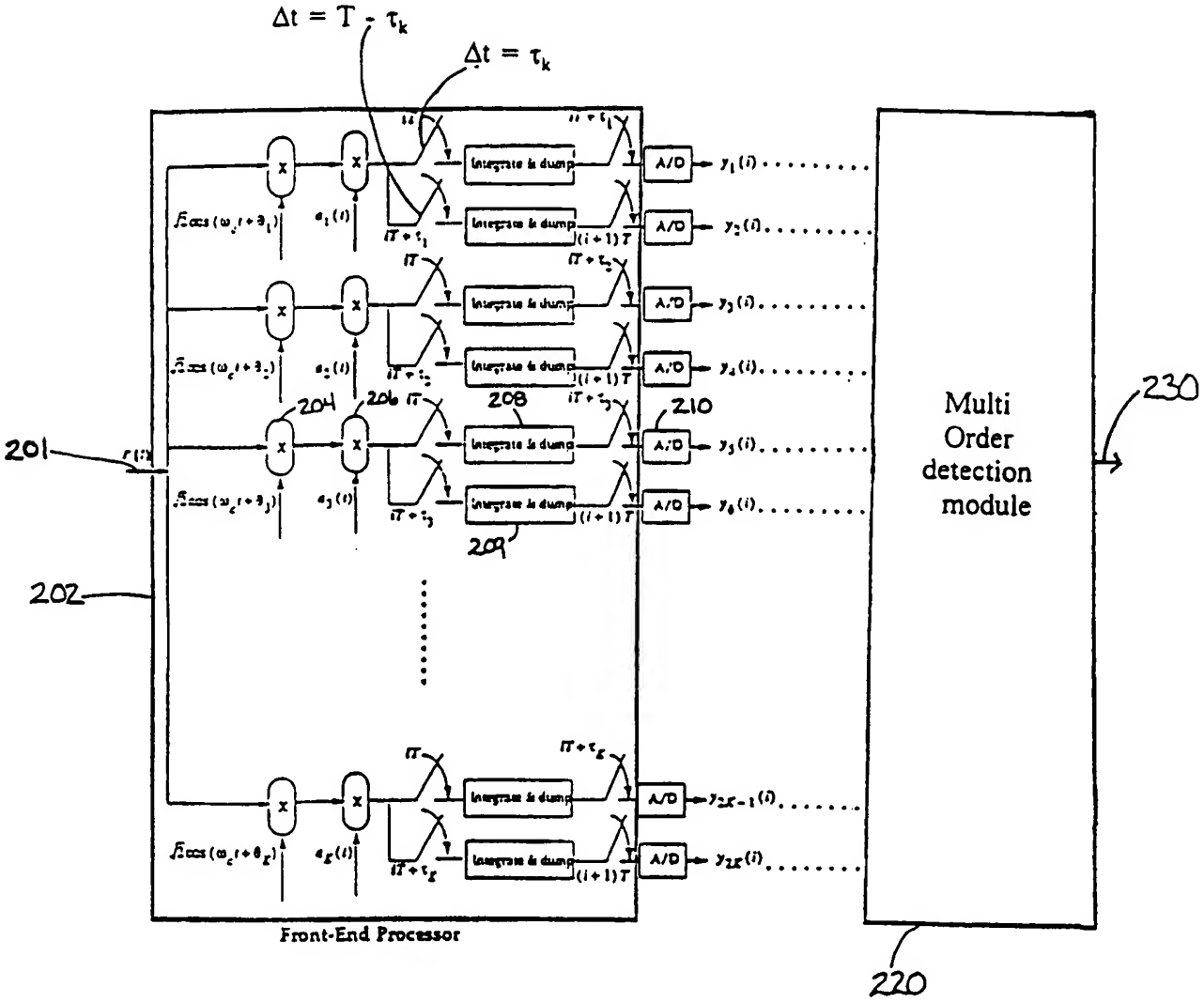
Δt = T - τk
Δt = τk
Integrate & dump
A/D
Multi Order detection module
Front-End Processor
201
202
204
206
208
209
210
220
230

Figure 2

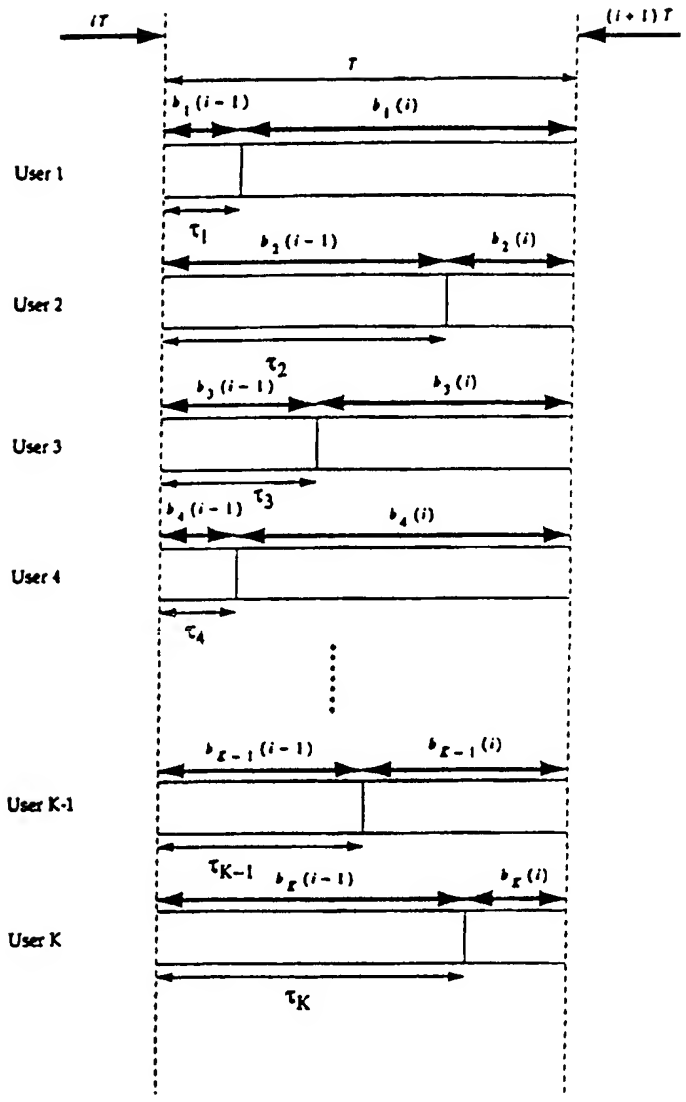

The delay of each user and the corresponding transmitted data symbols during observation time iT to $(i+1)T$.

Figure 3

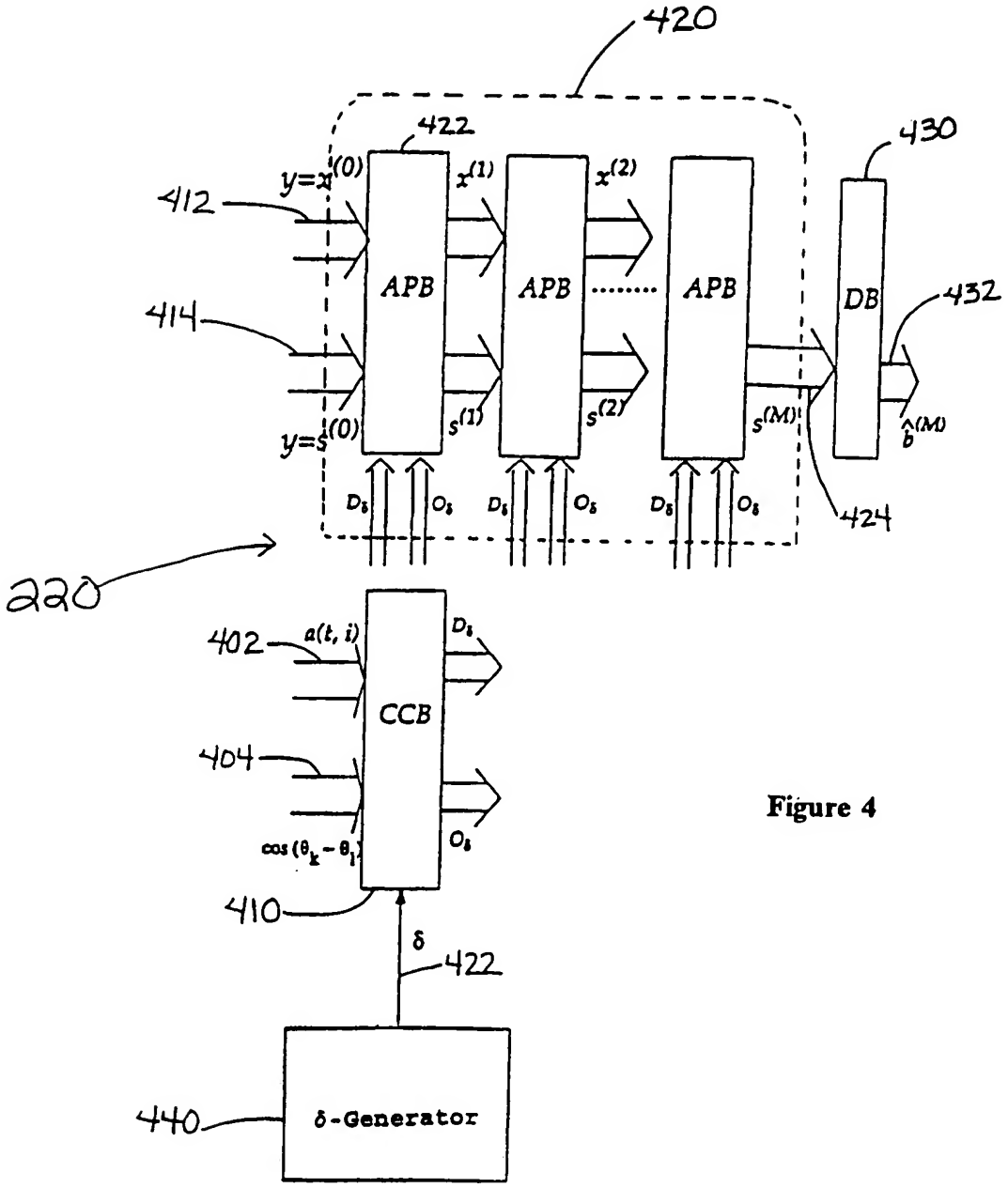

Figure 4

The δ-adjusted Mth order multiuser detector.

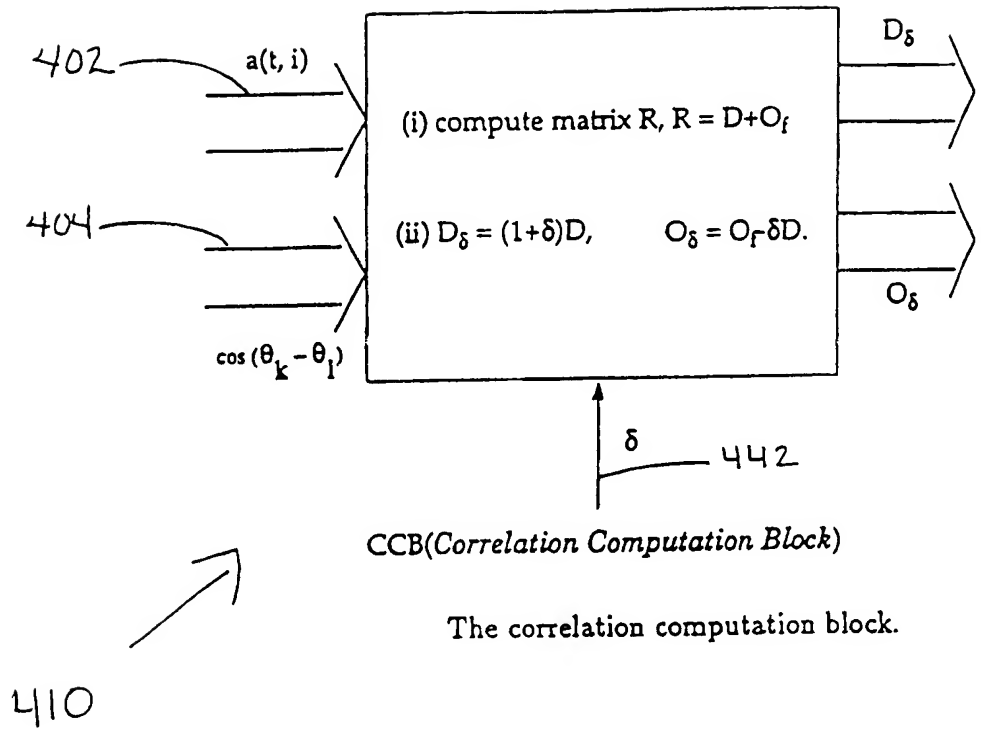

The correlation computation block.

Figure 5

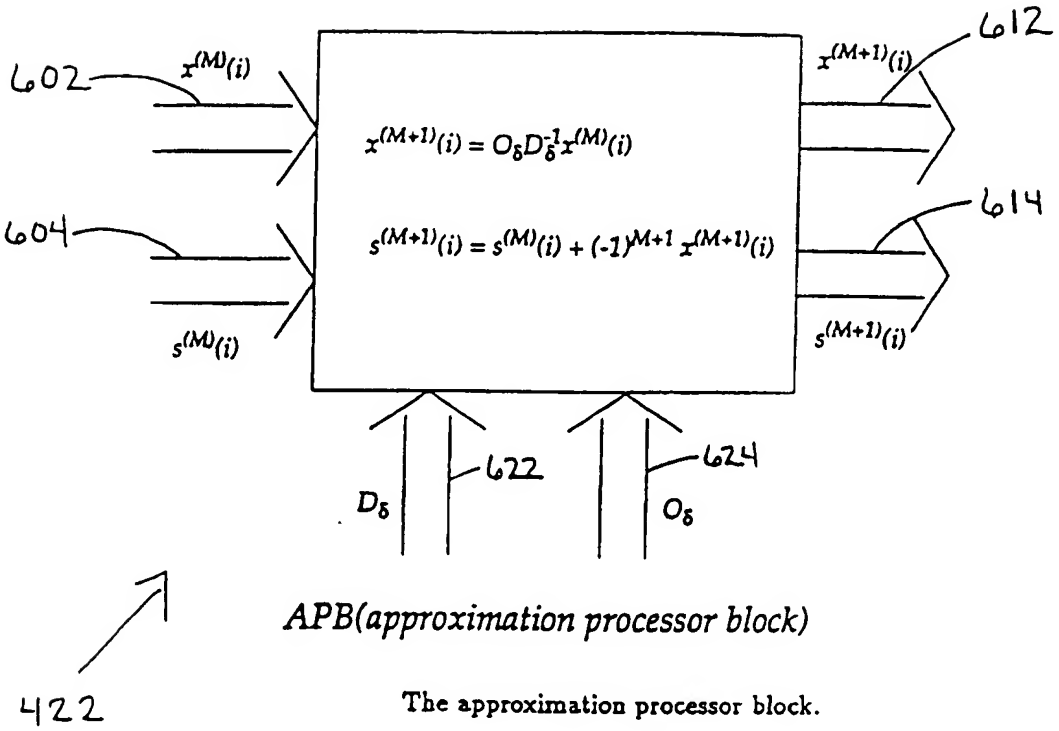

The approximation processor block.

Figure 6

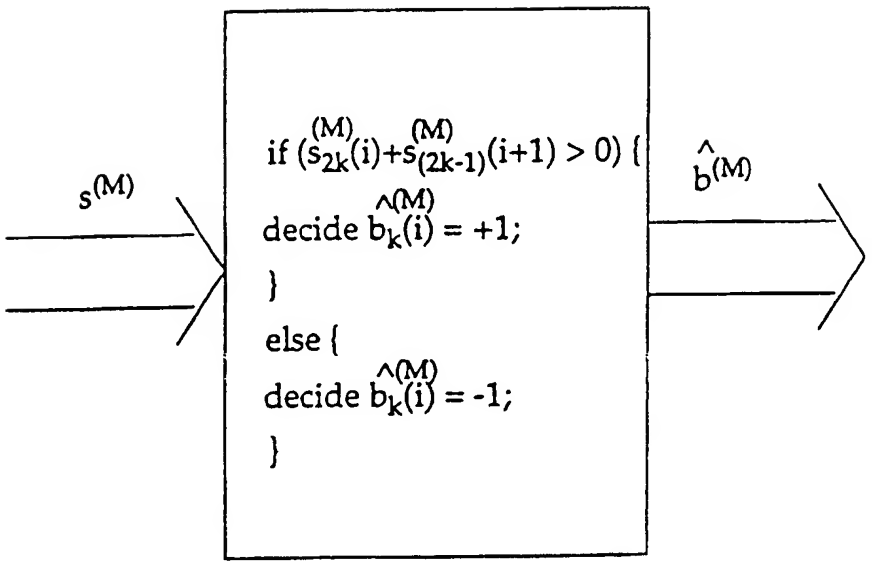

DB(*Decision Block*)

The decision block. 430

Figure 7

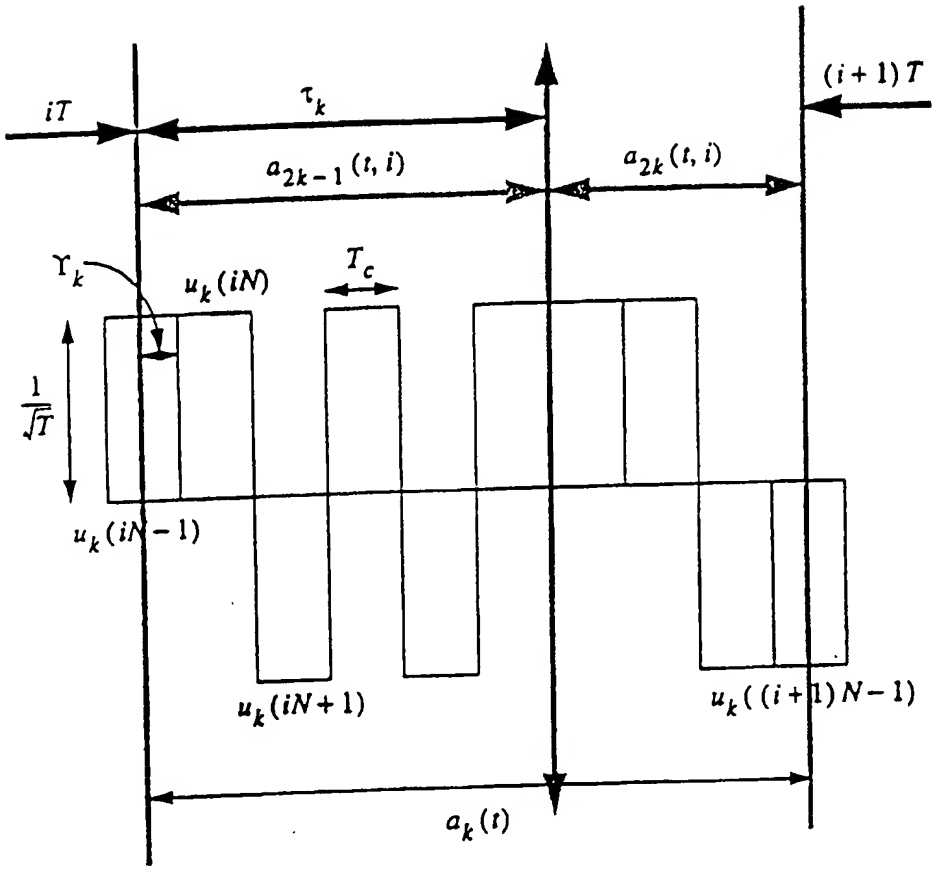

The kth user's spectral-spreading signal, $a_k(t)$, during the observation time iT to $(i+1)T$.

Figure 8

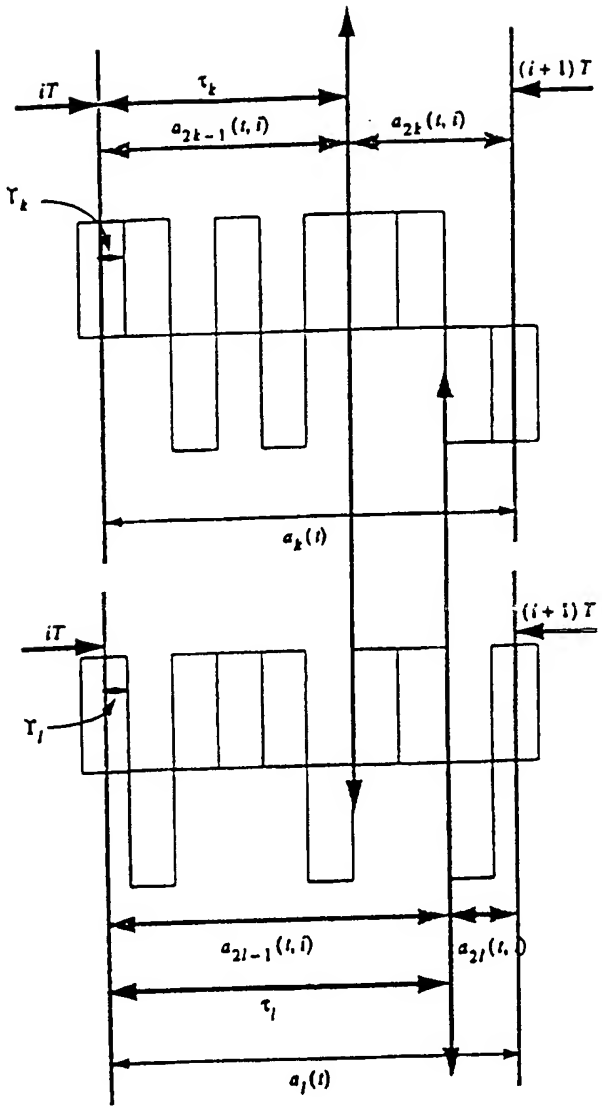

The spectral-spreading signals $a_k(t)$ and $a_l(t)$ when $\gamma_k = \gamma_l$ during the observation time iT to $(i+1)T$.

Figure 9

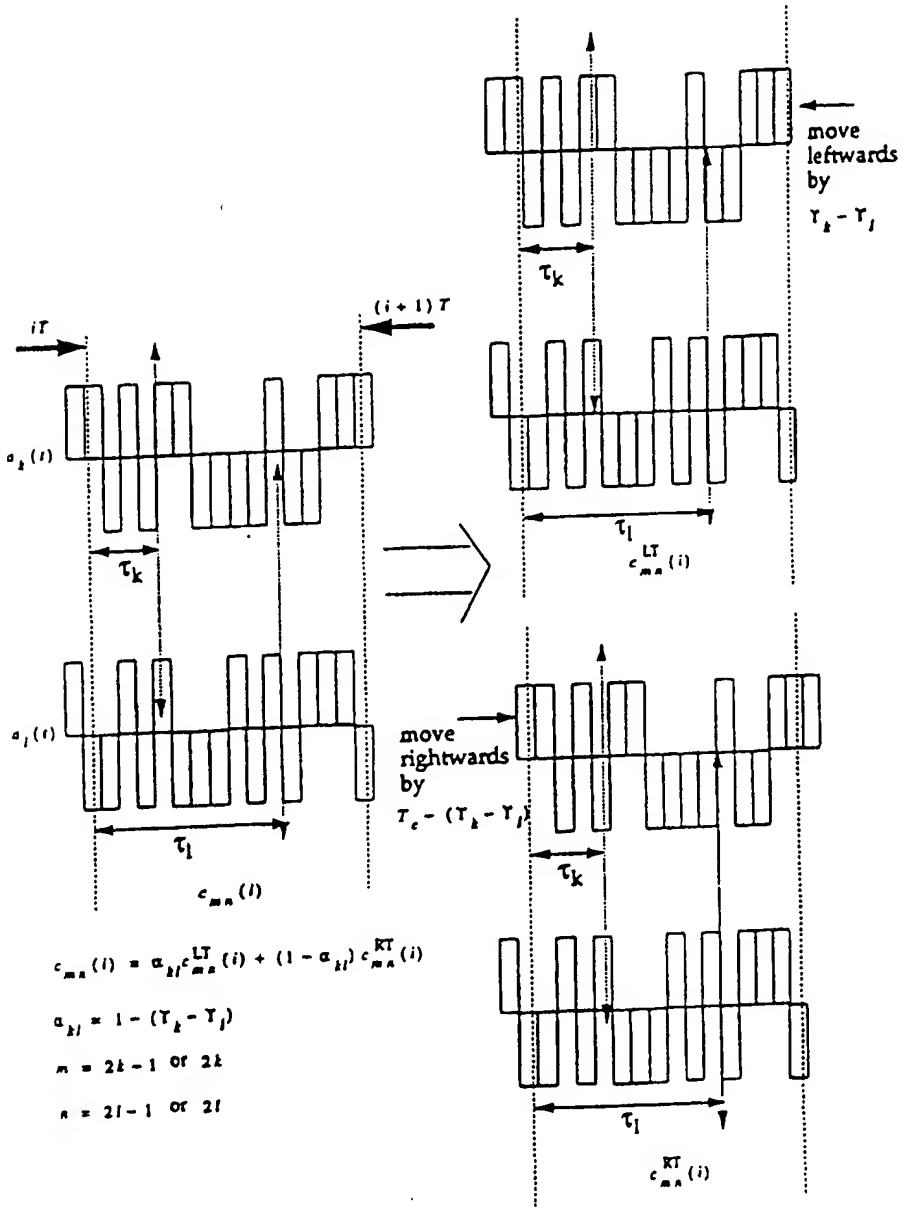

Computation of $c_{mn}(i)$ when $\gamma_k > \gamma_l$.

Figure 10

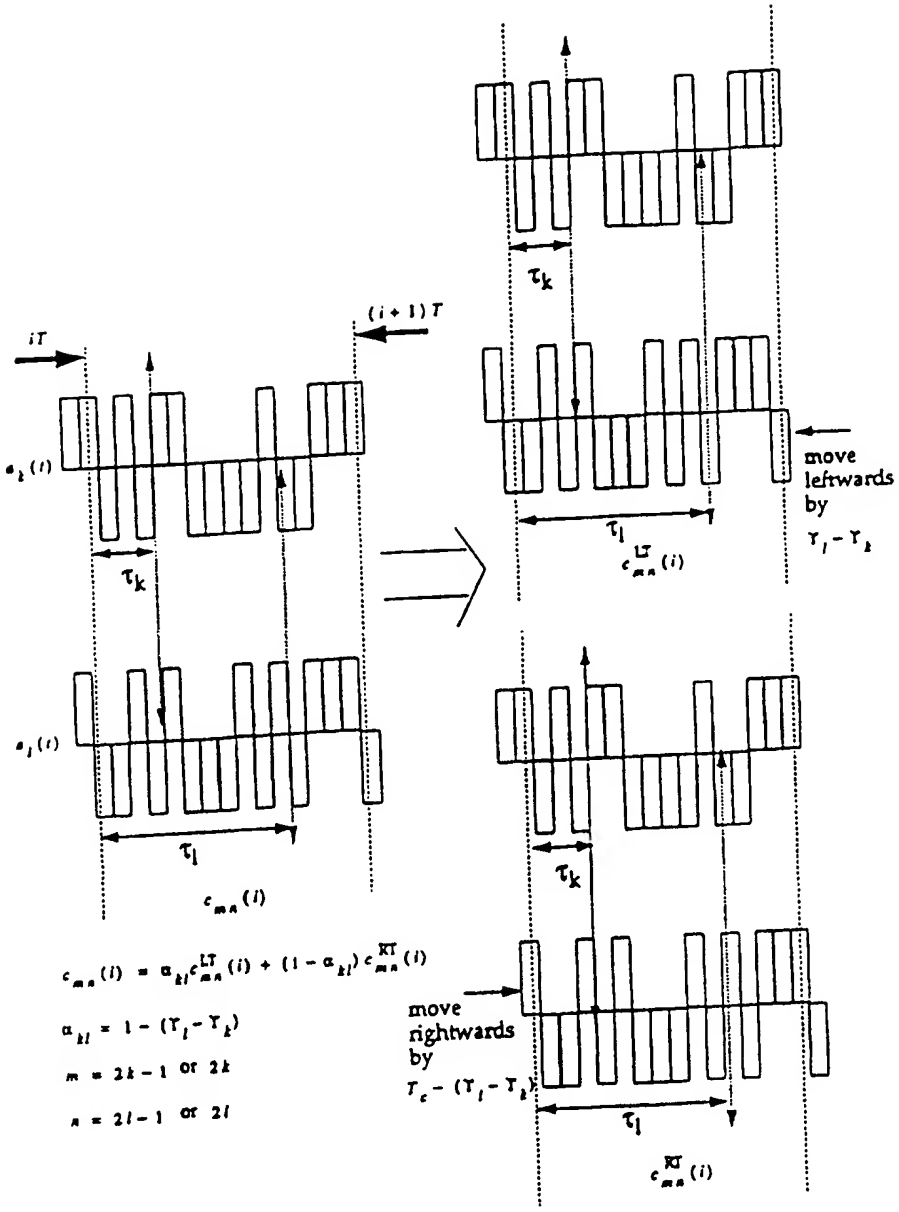

Computation of $c_{mn}(i)$ when $\gamma_k < \gamma_l$.

Figure 11

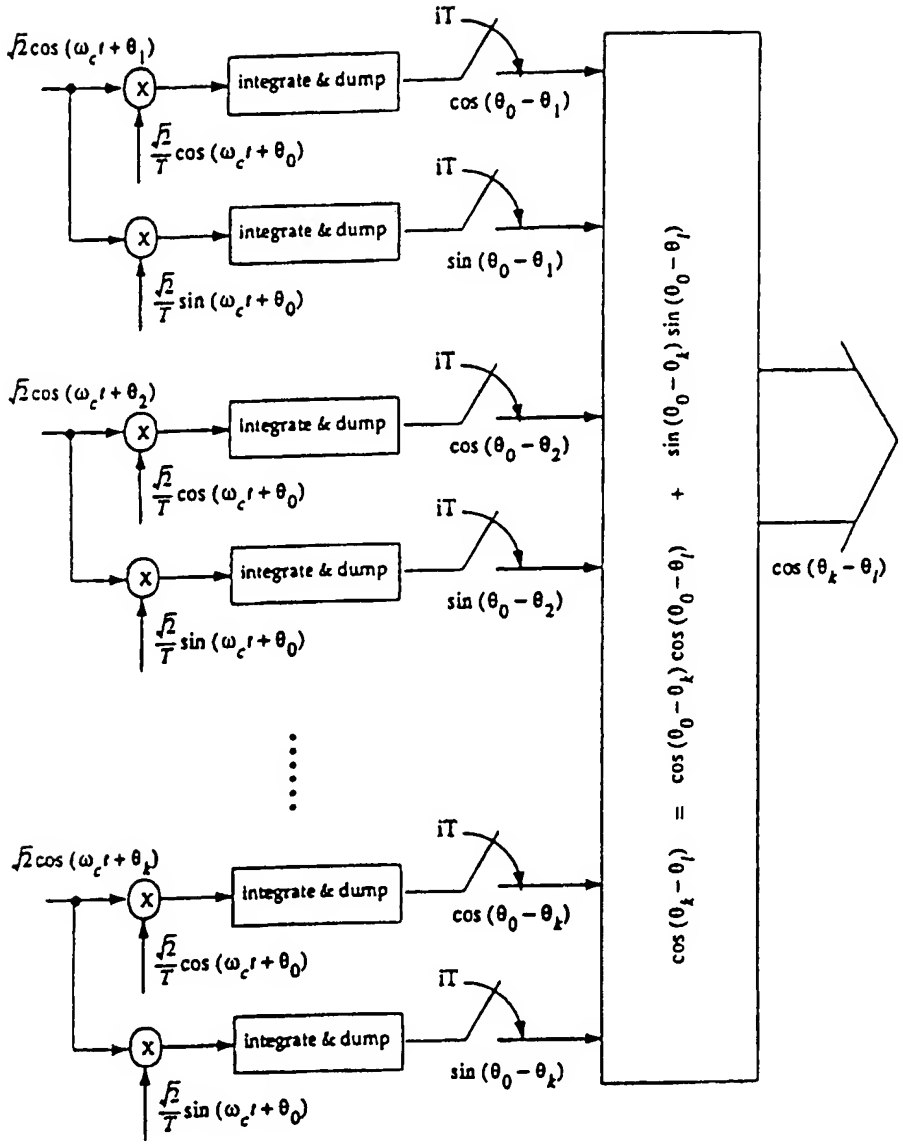

The derivation of $\cos(\theta_k - \theta_l)$.

Figure 12

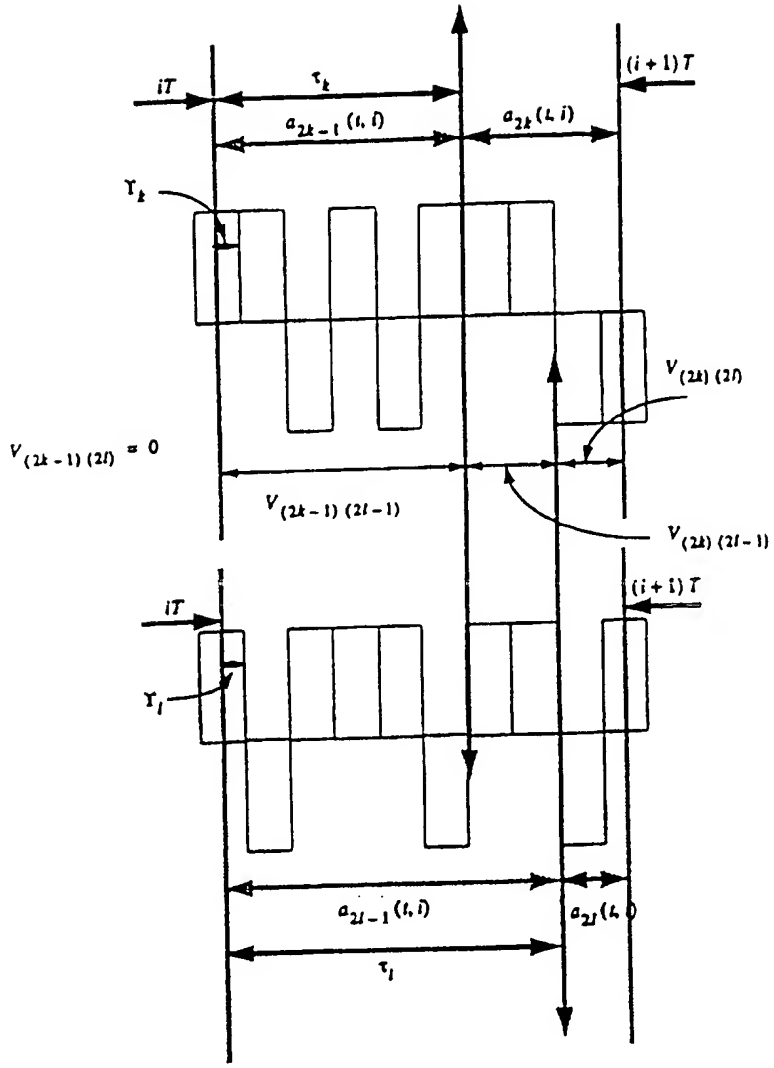

The magnitude of $V_{(2k-1)(2l-1)}$, $V_{(2k-1)(2l)}$, $V_{(2k)(2l-1)}$ and $V_{(2k)(2l)}$ when $\tau_k \leq \tau_l$

Figure 13

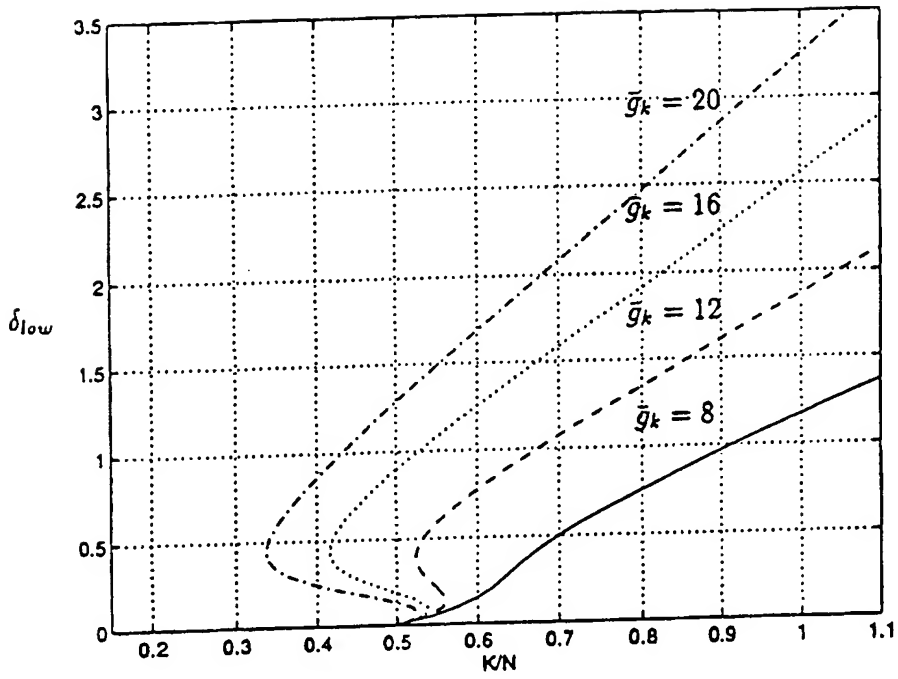

The exact value of δ_{low} for $\beta_k = 0$ dB.

Figure 14

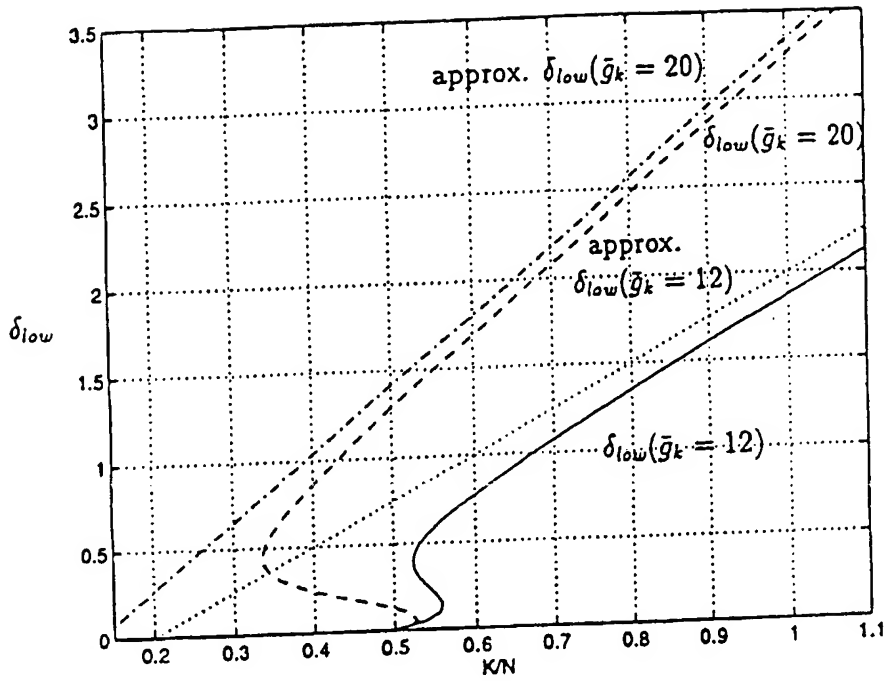

Comparison of the exact value and the approximated value of δ_{low}.

Figure 15

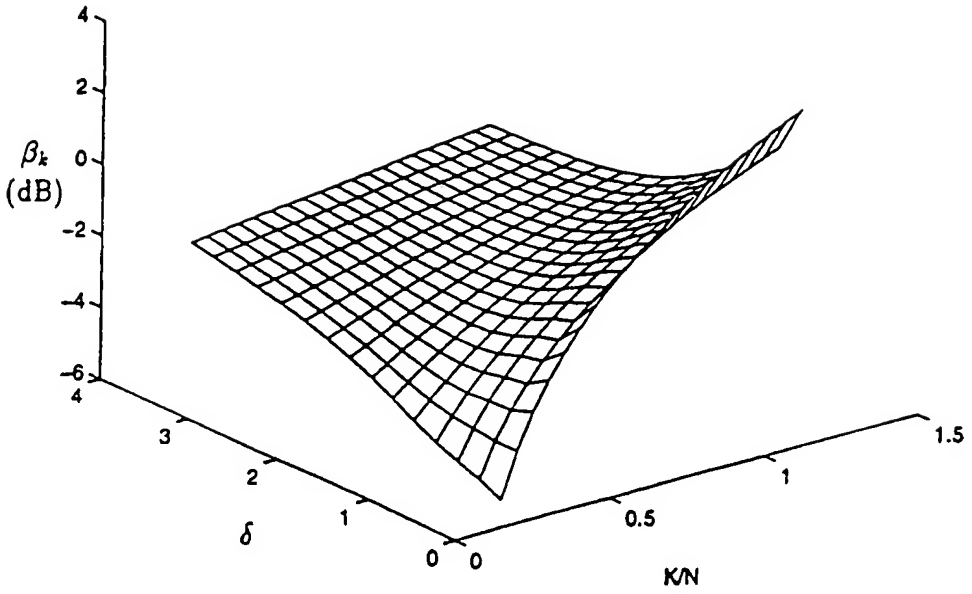

The β_k in dB versus K/N and δ when $\bar{g}_k = 8$.

Figure 16

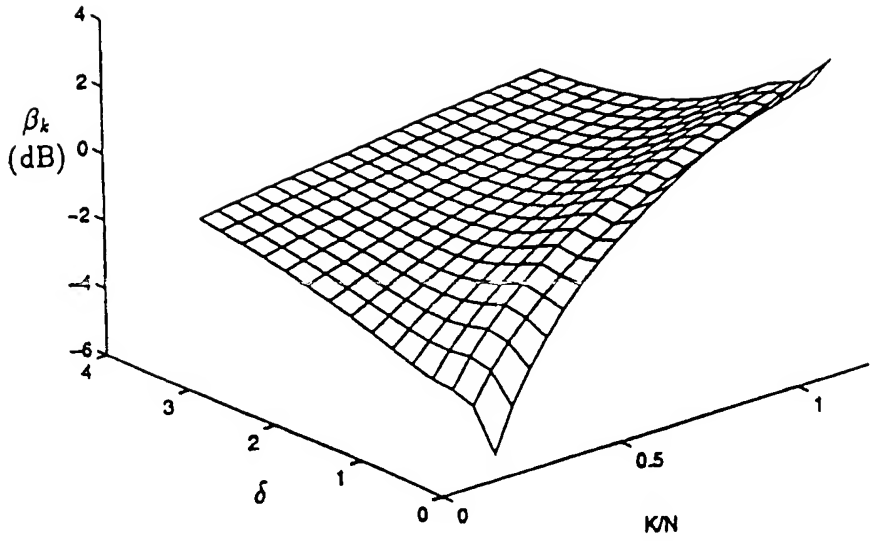

The β_k in dB versus K/N and δ when $\bar{g}_k = 12$.

Figure 17

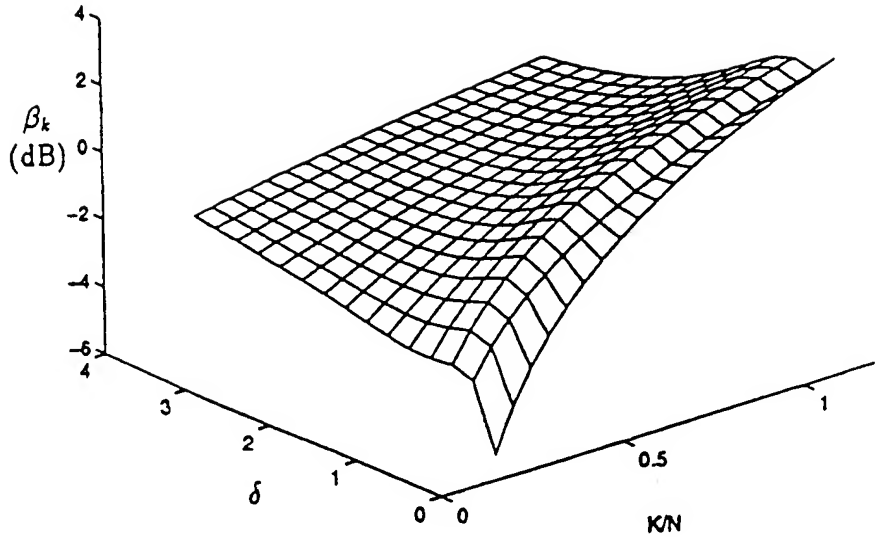

The β_k in dB versus K/N and δ when $\bar{g}_k = 16$.

Figure 18

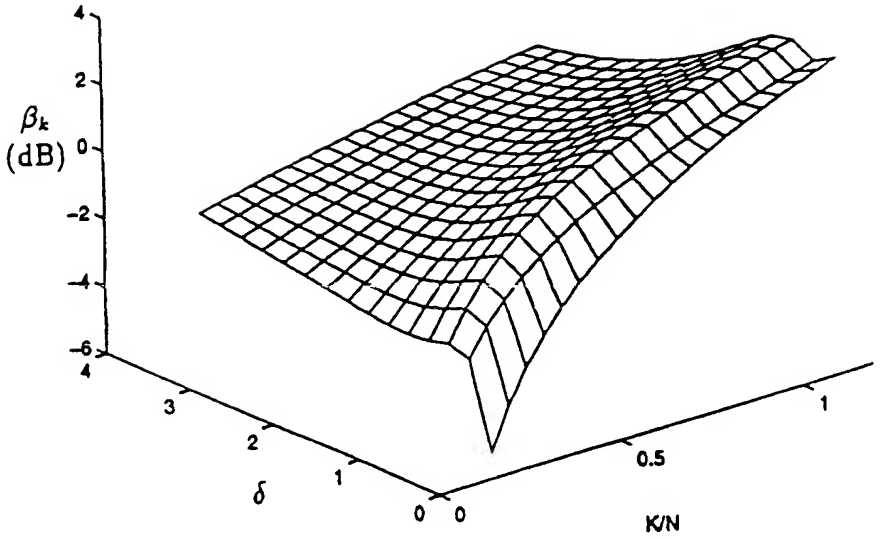

The β_k in dB versus K/N and δ when $\bar{g}_k = 20$.

Figure 19

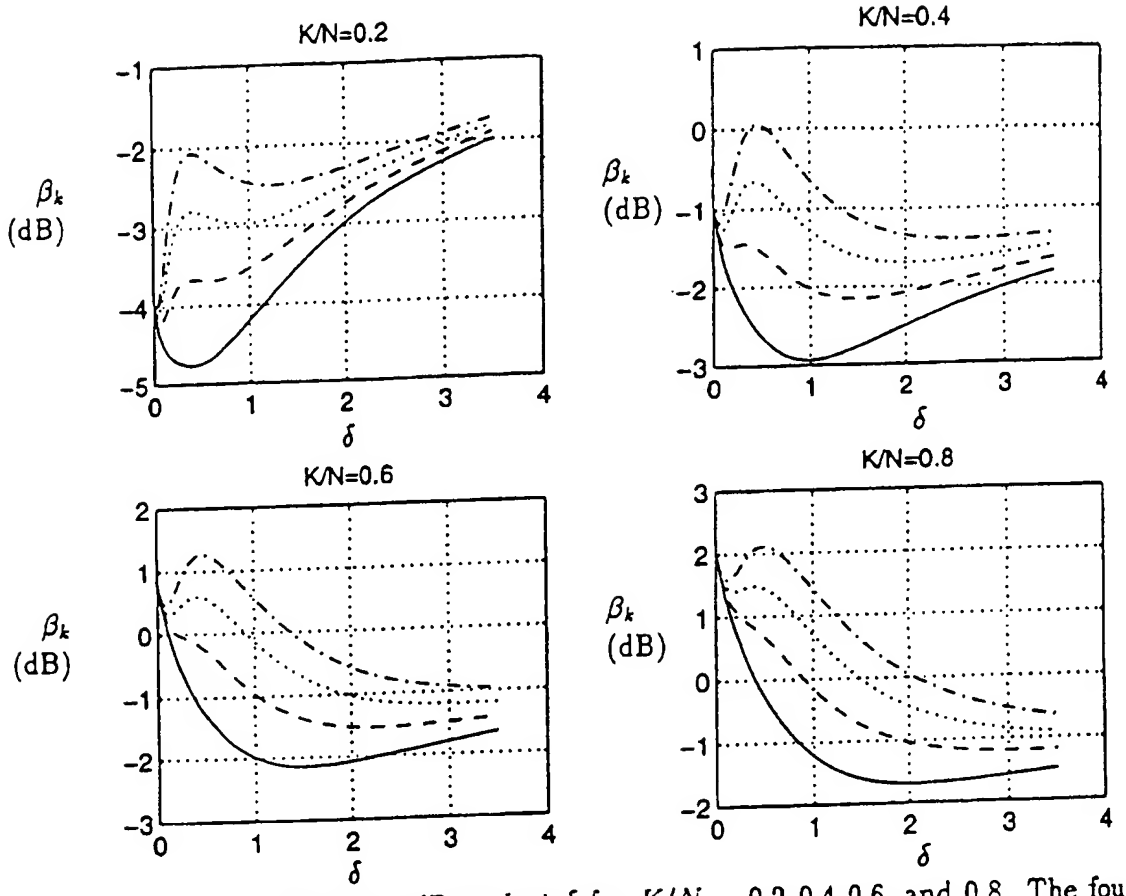

The β_k in dB against δ for $K/N = 0.2, 0.4, 0.6$, and 0.8. The four curves from the bottom up are for $\bar{g}_k = 4$ (solid line), $\bar{g}_k = 8$ (- - -), $\bar{g}_k = 12$ (...), and $\bar{g}_k = 16$ (-.-), respectively.

Figure 20

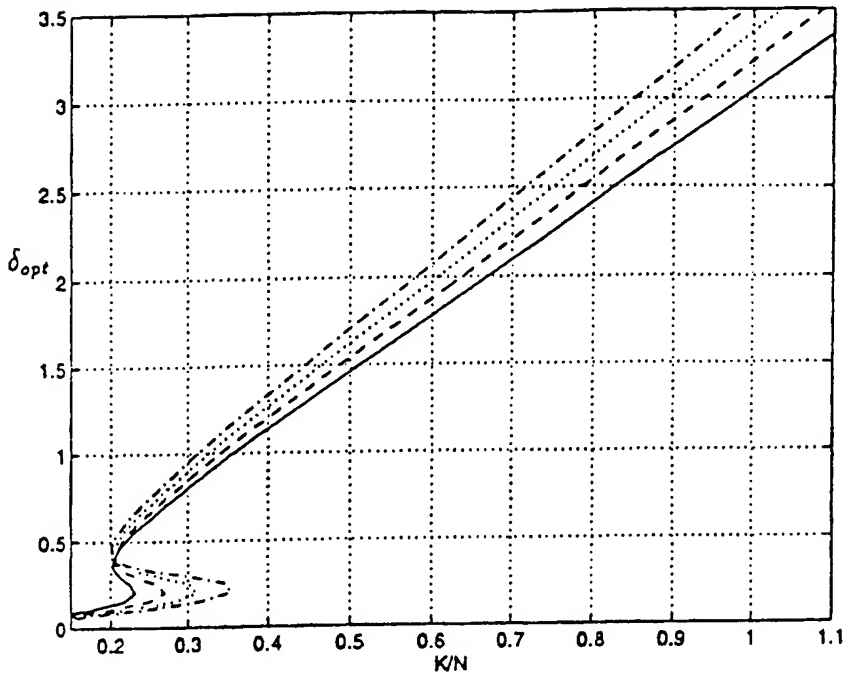

The contour for δ_{opt}. The four curves from the bottom up are for $\bar{g} = 6.4$ (solid line), $\bar{g} = 6.9$ (- - -), $\bar{g} = 7.4$ (...), and $\bar{g} = 7.9$ (-.-), respectively.

Figure 21

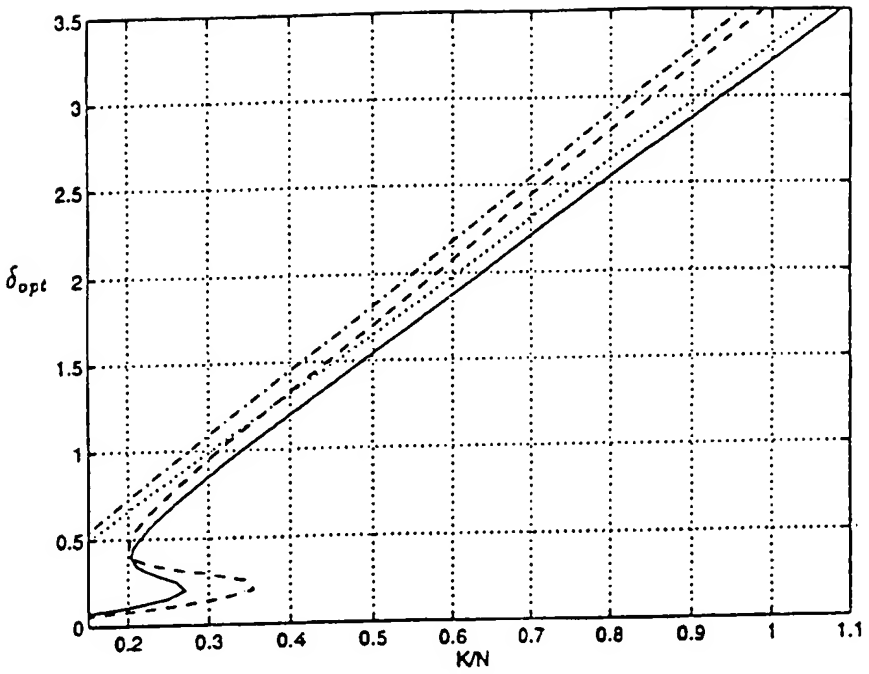

The contour for the exact value and the approximated value of δ_{opt}. The four curves from the bottom up are the exact contour with $\bar{g} = 6.9$ (solid line), the approximated contour with $\bar{g} = 6.9$ (...), the exact contour with $\bar{g} = 7.9$ (- - -), and the approximated contour with $\bar{g} = 7.9$ (-.-), respectively.

Figure 22

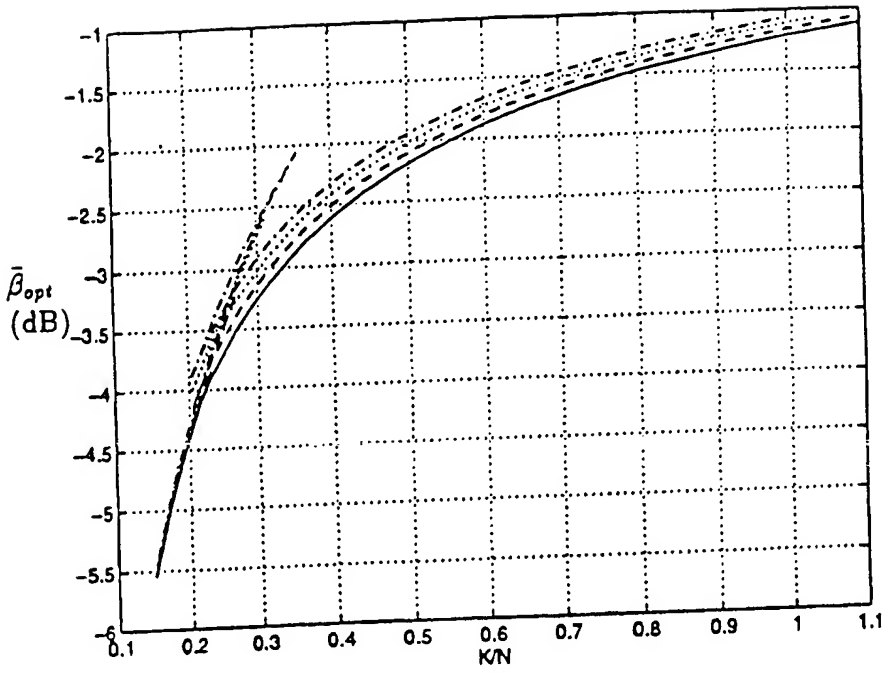

. $\bar{\beta}_{opt}$ in dB. The four curves from the bottom up are for $\bar{g} = 6.4$ (solid line), $\bar{g} = 6.9$ (- - -), $\bar{g} = 7.4$ (...), and $\bar{g} = 7.9$ (-.-), respectively.

Figure 23

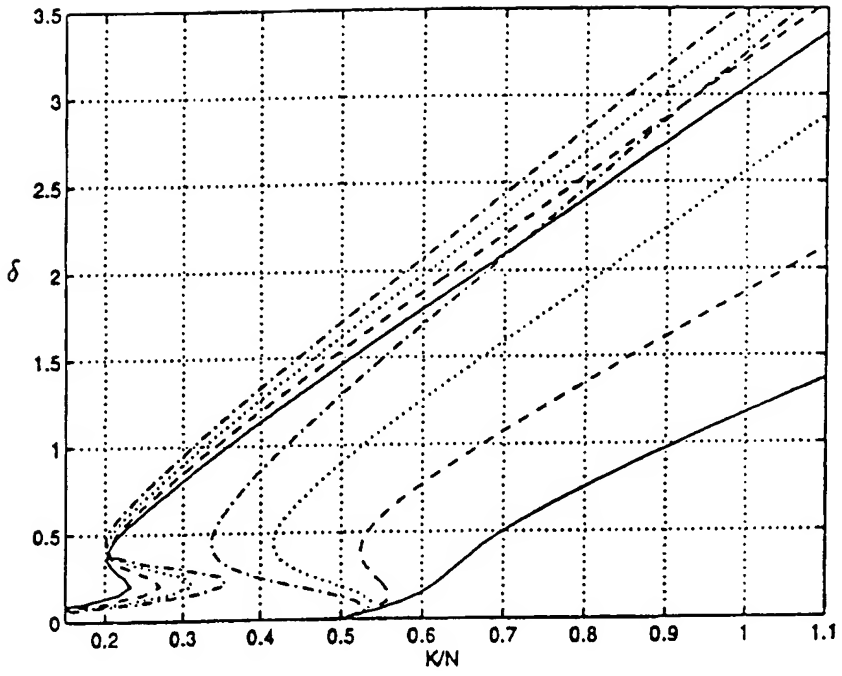

Comparison of δ_{low} and δ_{opt}.

Figure 24

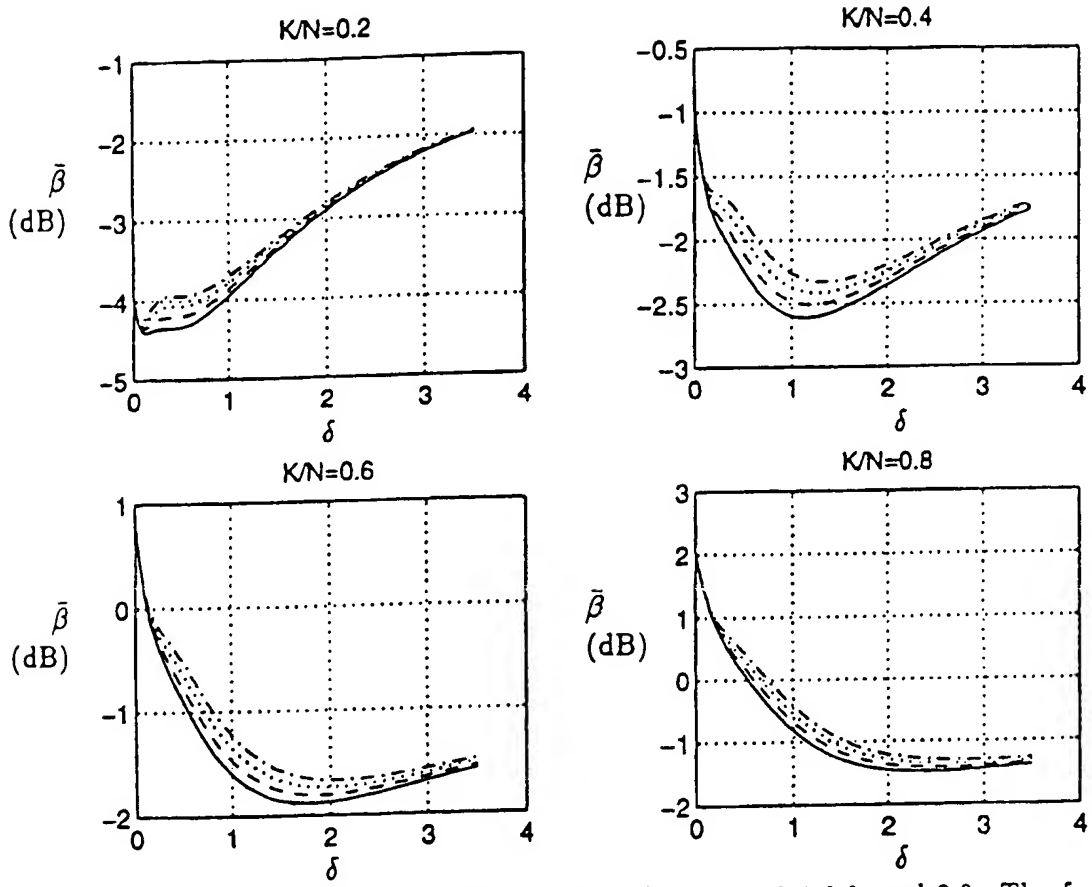

The $\bar{\beta}$ in dB against δ for $K/N = 0.2, 0.4, 0.6$, and 0.8. The four curves from the bottom up are for $\bar{g} = 6.4$ (solid line), $\bar{g} = 6.9$ (- - -), $\bar{g} = 7.4$ (...), and $\bar{g} = 7.9$ (-.-), respectively.

Figure 25

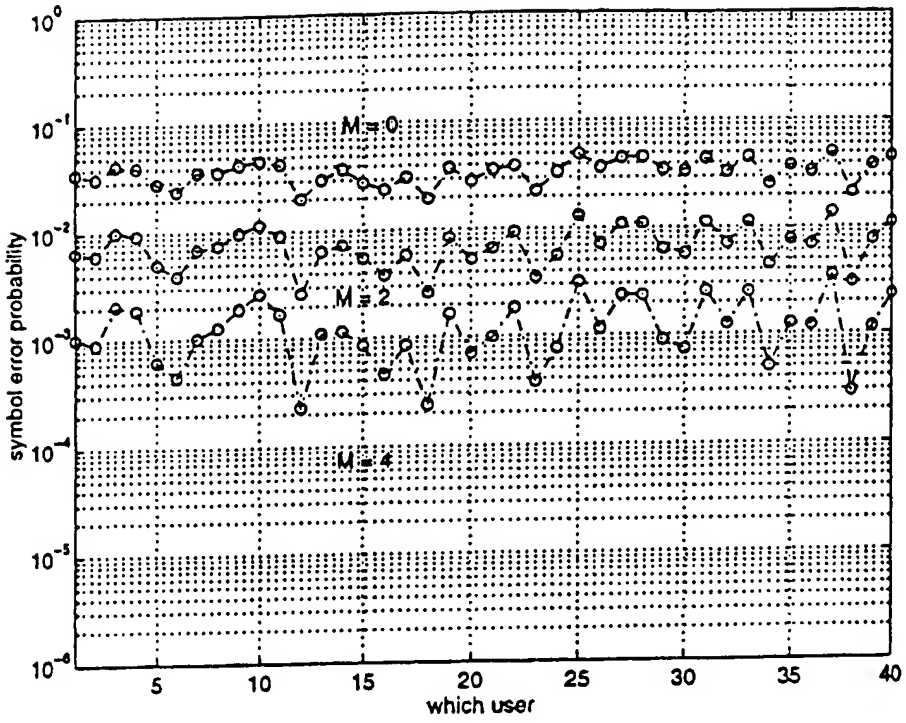

Symbol error probability for each user.

Figure 26

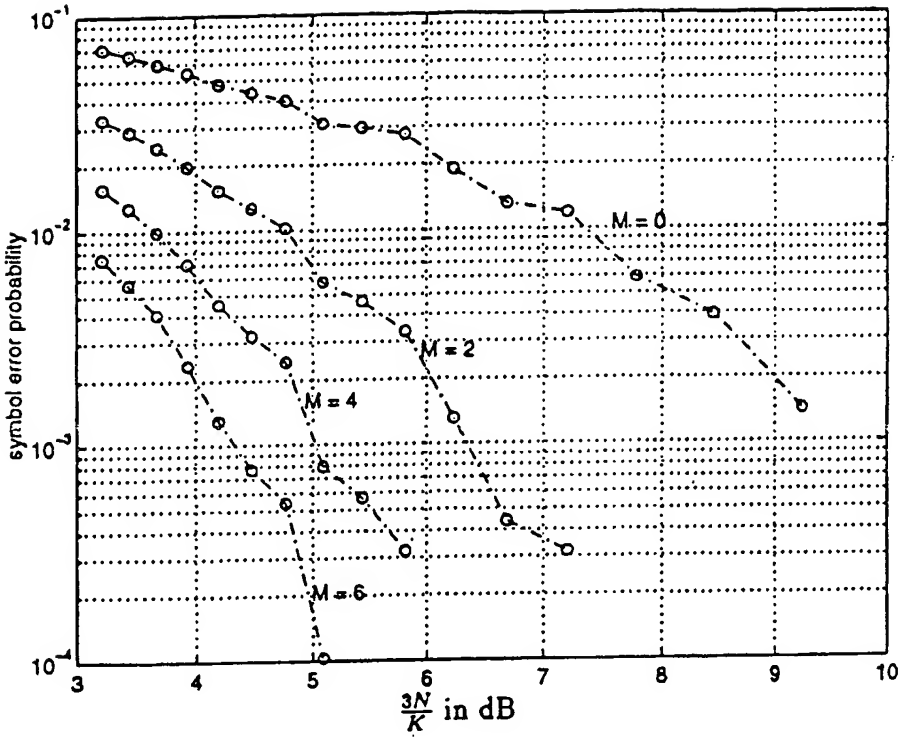

Average symbol error probability of all users versus $\frac{3N}{K}$ in dB.

Figure 27